Brain, Behavior, and Immunity 122 (2024) 150–166

Contents lists available at ScienceDirect

Brain Behavior and Immunity

journal homepage: www.elsevier.com/locate/ybrbi

Peripheral, but not central, IGF-1 treatment attenuates stroke-induced cognitive impairment in middle-aged female Sprague Dawley rats: The gut as a therapeutic target

Yumna El-Hakim [a], Kathiresh Kumar Mani [a], Kaylin A. Pickle [a], Zara Akbari [a], Nadia Samiya [a], Chloe Pham [a], Gianna Salas [a], Rachel Pilla [b], Farida Sohrabji [a,*]

[a] Women's Health in Neuroscience Program, Department of Neuroscience and Experimental Therapeutics, College of Medicine, Texas A&M University-Health Science Center, Bryan TX-77807 USA

[b] Department of Small Animal Clinical Sciences, College of Veterinary Medicine Texas A&M University, College Station, TX Brazos

A B S T R A C T

Stroke results in immediate sensory or motor disability and increases the risk for long term cognitive-affective impairments. Thus, therapies are urgently needed to improve quality of life for stroke survivors, especially women who are at a greater risk for severe stroke after menopause. Most current research on stroke therapies target the central nervous system; however, stroke also impacts peripheral organ systems. Our studies using acyclic (estrogen-deficient) middle aged female Sprague Dawley rats show that this group not only displays worse outcomes after stroke as compared to adult females, but also has lower levels of the neuroprotective peptide Insulin-like Growth Factor (IGF1) in circulation. Intracerebroventricular (ICV) administration of IGF1 to this group decreases infarct volume and improves sensory motor performance in the acute phase. In this study, we show that, despite this neuroprotection, ICV-IGF1 did not reduce peripheral inflammation or improve post stroke cognitive impairment in the chronic phase. In view of the evidence that stroke induces rapid gut dysfunction, we tested whether systemic delivery of IGF1 (intraperitoneal, IP) would promote gut health and consequently improve long-term behavioral outcomes. Surprisingly, while IP-IGF1, delivered 4 h and 24 h after ischemic stroke, did not reduce infarct volume or acute sensory motor impairment, it significantly attenuated circulating levels of pro-inflammatory cytokines, and attenuated stroke-induced cognitive impairment. In addition, IP-IGF1 treatment reduced gut dysmorphology and gut dysbiosis. Our data support the conclusion that therapeutics targeting peripheral targets are critical for long-term stroke recovery, and that gut repair is a novel therapeutic target to improve brain health in aging females.

1. Introduction

Stroke is the second leading cause of death worldwide and results in chronic disability among 50 % of its survivors (Donkor, 2018). The long-term consequences, which include neuropsychiatric conditions such as depression and dementia, are more severe in women. Approximately 1/3rd of stroke patients develop post stroke depression (PSD) (Hackett and Pickles, 2014) and a recent metanalysis of 47 studies showed that women are more likely to be afflicted with PSD than men (Poynter, 2009). Additionally, more than 50 % of patients suffer from some level of post stroke cognitive impairment (PSCI) (Jacquin, 2014; Mellon, 2015) by 6 months post stroke. Female sex is strongly associated with PSCI (Pendlebury and Rothwell, 2009), with women more likely to need assisted-living facilities as a result of deteriorating cognitive function (Bushnell and McCullough, 2014; Bushnell, 2014; Gall et al., 2012). These data underscore the urgent need for effective therapies for the middle-aged female demographic.

While the elevated risk for stroke and stroke severity in women is usually associated with declining levels of ovarian hormones after menopause, there is also an age-related decline in the levels of other endocrine factors. For example, circulating levels of the peptide hormone insulin-like growth factor (IGF1) decrease with age (Waters et al., 2003) and low levels of IGF1 are predicative of poor stroke outcomes (Bondanelli, 2006; Johnsen, 2005). In our previous studies, ICV delivery of IGF1 to acyclic middle-aged female rats, 4 h after stroke, reduced infarction, improved the neurological score, reduced blood brain barrier (BBB) permeability, and decreased expression of cytokines in the brain, indicating robust acute neuroprotection (Bake et al., 2014; Bake et al., 2019; Okoreeh et al., 2017). However, the impact of IGF1 treatment on the long-term consequences of stroke, such as PSD and PSCI have not been examined in this model.

The pathophysiology underlying post-stroke cognitive impairment is likely multifactorial. In addition to neuronal damage, stroke has been shown to induce aberrant patterns of axonal sprouting, decline in

* Corresponding author.
E-mail address: f-sohrabji@tamu.edu (F. Sohrabji).

https://doi.org/10.1016/j.bbi.2024.08.008
Received 24 August 2023; Received in revised form 18 July 2024; Accepted 8 August 2024
Available online 12 August 2024

synaptic plasticity and density (Corbett et al., 2006), damage to axons (Liu et al., 2008) and white matter tracts (Kalaria et al., 2016). Neuroimaging studies have shown that the effects of stroke are not confined to the local infarction site and can include structural and functional connectivity changes distal to the injury (Lim et al., 2021), a phenomenon called 'connectional diaschisis' (Carrera and Tononi, 2014). Cognitive domains that are affected may also vary with stroke characteristics such as stroke type, infarct volume, location, and severity (Kalaria et al., 2016). More recent studies show that cognitive complications can become exacerbated after injury due to brain and systemic inflammatory responses. A *meta*-analysis indicated that AD and related dementia are accompanied by high peripheral levels of several cytokines including IL-6, TNF-α, IL-1β, TGF-β, IL-12, IL-17A and IL-18 (Swardfager, 2010; Lai, 2017). IL-17A, which is implicated in the pathogenesis of several neurological diseases in human and animal models, is produced by T cells including Th17 and γδ-T cells which are enriched in the gut lumen and can extravasate to the brain after stroke (Brea, 2021). Our previous studies show that ICV-IGF1 decreases stroke-induced elevation of inflammatory cytokines in the ischemic hemisphere (Bake et al., 2014), however, its effects on levels of circulating inflammatory cytokines are unknown.

The current study was therefore designed with a dual purpose: the first was to examine whether ICV-IGF1 would also promote cognitive health in the chronic phase. The second goal was to test whether a more clinically tractable route of administration for IGF1 such as intraperitoneal (IP) would also be effective for stroke neuroprotection. We report that while ICV-IGF1 was neuroprotective in the acute phase, this treatment failed to improve cognitive outcomes in the chronic phase. In contrast, IP-IGF1 was not neuroprotective in the acute phase, but successfully ameliorated stroke-induced elevations in inflammatory cytokines and cognitive impairment. Our data further show that IP-IGF1 treatment reduced stroke-induced intestinal dysmorphology, and permeability as well as gut dysbiosis, implicating gut repair as a critical target for long term improvement of stroke outcomes.

2. Methods

2.1. Animals

Middle-aged (12 month old) female Sprague Dawley rats were purchased from Envigo Laboratories (IN) and maintained in a constant 12-h dark: 12-h light cycle with *ad libitum* food and water. All rat procedures were reviewed and approved by the Texas A & M University Institutional Animal Care and Use Committee in accordance with OLAW guidelines for the humane treatment of animals in research. STAIR recommendations were followed including the use of aging animals, random group assignment, blind testing conditions, acute and long-term studies, and the use of multiple behavioral tests (Saver, 2009). Daily vaginal smears were obtained to confirm that middle-aged females were acyclic (Jezierski and Sohrabji, 2001). Rats were randomly assigned to the following groups in the ICV studies: Sham (no MCAo) with vehicle ICV infusion (vehicle-aCSF), MCAo with vehicle ICV infusion, and MCAo with IGF1 ICV infusion. Vehicle or IGF1 infusion was initiated 4 hr post stroke for 48 h as described in (Bake et al., 2014). Briefly, Alzet osmotic minipumps (1007D, Alzet corp., CA, flow rate 0.5 μl/h, reservoir volume of 96 ± 2 μl) was loaded with human recombinant (rh)IGF-1 (R&D Laboratories, 100 μg/ml), primed overnight and placed into a subcutaneous pocket between the scapula and spine. Rats were randomly assigned to the following groups in the IP studies: Sham (no MCAo) with vehicle IP injections (vehicle-PBS), MCAo with vehicle IP injections, and MCAo with IP-IGF1 injections. Vehicle or IGF1 IP injections (200 μg) were given 4 and 24 h after stroke. This dose was selected based on published reports where rhIGF1 was administered systemically, and tested empirically by us in a small pilot study. Recombinant human IGF1 (R&D systems, 291-G1-01 M) was used in all studies. All animals were fed pelleted food (Harlan 8604 Teklad diet) for at least 4 weeks prior to their assignment to the study. In all, 136 middle aged females were used in these studies, distributed as follows: 48 middle aged females were used in the IP (n = 24) and ICV (n = 24) acute studies (6 sham, 8 vehicle and 8 IGF1 in each case), 38 animals (8 sham, 15 vehicle and 15 IGF1) were used for the chronic IP study and 36 animals (7 sham, 15 vehicle and 14 IGF1) were used for the chronic ICV study. An additional 12 animals were used in the dextran assay.

2.2. Middle cerebral artery occlusion

Animals were subjected to stereotaxic surgery to occlude the left middle cerebral artery as reported in (Selvamani and Sohrabji, 2010; Selvamani and Sohrabji, 2017). Briefly, endothelin-1 (3 μl, 1:2 dilution in DPBS of 1 mg/ml endothelin-1 stock; American Peptide Company, Inc., CA) was injected adjacent to the middle cerebral artery at the following stereotaxic coordinates relative to bregma: + 0.9 mm anterior/posterior, + 3.4 mm medial/lateral, and − 8.5 mm relative to the dura. The same procedure was followed for sham surgeries without the injection of endothelin-1. Stroke-induced mortality was 20.9 %.

2.3. Infarct volume

Infarct volume analysis was determined using our previous procedures (Selvamani and Sohrabji, 2010). Images were coded and infarct volume was measured using image analysis software, Image J (NIH, MD), by an experimenter who was blind to the codes. Total brain infarct was calculated from 3 slices per animal and expressed as the ratio of infarct volume in the ischemic hemisphere to the total volume of the non-ischemic hemisphere.

2.4. Behavioral analysis

All testing was performed between 9 am and 1 pm to minimize the contribution of circadian variations to behavioral performance. All tests were performed and scored by experimenters who were blind to the treatment condition. For assessing sensorimotor function, the adhesive tape removal test and the vibrissae evoked forelimb placement task was performed before (Pre, −2 days) and after (2 and 5 days) stroke. The animals were used for behavioral analysis 4 weeks after stroke. The sequence of behavioral testing was Social Interaction, Novel Object Recognition Task and Barnes maze test. In general, subsets of all the three groups (sham/Vehicle/IGF1) of animals were assessed on the same day for a particular behavioral test. For most assays, tests were performed pre and post stroke and analyzed by repeated measures. Due to multiple behavior tests, animals were not randomized by baseline values, but were compared pre and post using repeated measures analysis.

2.5. Sensory motor impairment tests

Sensory-motor impairment following MCAo was assessed using the vibrissae-evoked forelimb placement task (VIB) and the adhesive-tape removal test (ART) as described previously (Selvamani and Sohrabji, 2017; Selvamani et al., 1979; Balden et al., 2012). Both tests were performed prior to and 2 days and 5 days after the MCAo surgery to confirm cortico-striatal infarction. For the VIB task, the ipsi- or contralesional whiskers of the rat are stimulated on a surface and the reflexive placing of the paw upon that surface is scored. For the adhesive tape test, a piece of adhesive backed foam tape was used as tactile stimuli attached to the palmar surface of the paw of each forelimb in succession. For each forelimb, the time it took to remove the stimulus (tape) from the forelimbs was recorded during three trials per day for each forepaw. Animals were allowed to rest for 1 min between sessions, and each test session had a maximum time limit of 120 s.

3. Tests for depressive-like behavior

3.1. Social interaction test

A three-chambered Plexiglass box was used for the assessment of social interaction (Panta et al., 2019; Panta, 2020). Test animals were habituated in the apparatus for 5 min. Animals were returned to the home cage and were tested after an hour. For testing, a conspecific, naive adult same-sex stranger rat was placed within a plastic mesh cylinder in one of the end chambers, while the test rat was placed back in the middle chamber and allowed to explore for 10 min. The 10 min trials were video recorded for analysis. Sociability was scored as the total time (in seconds) spent by the test rat in the chamber with the stranger rat.

4. Tests of cognitive performance

4.1. Novel object recognition task (NORT)

The object recognition memory was tested as described previously (Panta et al., 2019; Panta, 2020). The animals were habituated in a plexiglass chamber (16″ × 16″) and then trained with two identical objects (odor-free plastic animal toys), (A+A) placed in opposite corners of the chamber, for 10 min. Animals were returned to the home cage and were tested after an hour. For testing, animals were placed in the chamber with two objects in the same location as before, one that was previously available (A) and the other that was novel (B). The 5 min trials were video recorded for the analysis. The amount of time spent exploring the novel object was determined during the first minute from these recordings by an investigator blind to the experimental condition. Exploration of an object was defined as the animal's snout directed to the object, sniffing or touching the object with its snout at a distance < 2 cm to the object and/or touching it with the nose. The discrimination index was calculated as follows: DI: [time spent with novel object]-[time spent with familiar object]/[time spent with novel object] + [time spent with familiar object]. Animals that showed a clear preference for the novel object (DI>0.1) in the baseline test were included in subsequent analysis.

4.2. Barnes maze

This test was performed to assess spatial learning and recall as described previously (Rosenfeld and Ferguson, 2014). A circular maze (diameter of 48″) consisting of 20 holes was used. Each hole consisted of either a small square box (19 total; 4″ × 4″ × 2″) or one bigger escape box (8″ × 4″ × 4″). The test was divided into two phases spanning 8 days: habituation (1 day) and learning (3 days), a 2-day break and then a probe trial (1 day). For habituation, rats were placed in the escape box for 2 min covered with a lid. After 2 min in the escape box, rats were placed inside a dark tube at the center of the Barnes maze. Bright lights (for aversion) were turned on and the center tube gently lifted off allowing the rats to freely explore the maze for a maximum of 5 min to find the escape box. If the rat did not find or enter the escape box in 5 min during the day of habituation, the experimenter manually guided the rat to the escape box. Once the rat entered the escape box, lights were turned off. The next day, during the learning phase, the escape box was placed at a fixed location under the escape hole (goal), and the rats were allowed a maximum of 2 min to find the escape. Each rat underwent three trials at an interval of 15 min, every day for 3 days. After a two-day break, a probe trial was performed where the escape box was replaced with a small square box and the rat explores the maze for 2 min. Ethovision software (Noldus) was used to analyze the latency to find the escape box as well as velocity and distance traveled during each trial. Following spatial acquisition, a probe test was conducted for 60 secs with no escape box to assess the spatial reference memory. The Ethovision software was used to analyze the time spent in the "target quadrant" where the escape box was located during the learning portion of the test.

4.3. Brain volumetric analyses

For the long-term study, animals were anesthetized and perfused transcardially with saline followed by 4 %paraformaldephyde. Brains were removed from the cranial vault and post-fixed for 24 h. Brains were then shipped to NeuroScience Associates (Knoxville, TN) for block embedding and sectioning. One set of sections was stained for Weil myelin, using the protocols standardized by NSA. Stained slides were imaged at 20x magnification using an Olympus VS120 Slide Scanner. For each section between bregma 2.52 and −5.88, the ipsilateral or contralateral hemisphere was manually outlined and measured on the open-source software QuPath (0.4.3) to obtain an area measurement (μm^2). The sum of cross-sectional areas was then multiplied by slice thickness (30 μm) and the number of slides between starting and ending bregma points (ranging from 19 to 22 sections) to obtain a volume measurement (μm^3). Lateral ventricle volume in each hemisphere was calculated as above using slices between approximate bregma 1.56 and −5.88. The thickness of the corpus callosum was measured to determine the extent of white matter damage after ischemic stroke.

For each brain, 5 sections of the corpus callosum (0.6 mm apart; approximate bregma 0.3 mm to − 0.9 mm) were assessed using a protocol described in Challa et al. (Challa, 2024). The dorsal to ventral margin of the corpus callosum was measured at the midline of each section using QuPath software and was averaged across 5 sections.

4.4. ELISA assays

Serum was collected via saphenous draw at baseline and 2 days and 5 days post-stroke. ELISA assays were used to determine LPS (Mybiosources, MBS268498), MUC-2 (Mybiosources, MBS 2019254), and iFABP (Mybiosources, MBS3807789). In addition, an ELISA assay for human IGF1 was performed on blood samples and brain from the IP study to assess circulating levels of rhIGF1. For all ELISA, the procedure was performed according to the manufacturer's directions and our published procedures (Park and Sohrabji, 2016; Bake et al., 2017). Plates were read on a microplate reader (450 nm; TECAN, VT) and the concentration of the samples was obtained by interpolation from the standard curve. Inflammatory cytokine/chemokine in the serum were quantified using a rat cytokine/chemokine multianalyte panel (Millipore, MA). The procedure was performed according to the manufacturer's directions and our published procedures (El-Hakim, 2021).

Gut health was assessed by a set of measures that have been shown to be affected by stroke. This includes routine histology (H&E staining), Periodic Acid Shiff staining, lectin histochemistry, dextran assays for gut permeability, fecal microbiome analysis and SCFA levels.

4.5. Gut histology

Gut histology focused on the distal ileum, a region where we have observed severe morphological changes after stroke (Bake et al., 2017; Kulesh et al., 2018). The ileum is a major site of nutrient absorption, immunological function (access and transfer of antigens) and therefore, a site where permeability is well-regulated. Based on these features, a 4 cm portion of the distal ileum was dissected using the cecum as a reference point and embedded in Cryo-OCT compound. For the acute (2d) time point, sections were collected from deeply anesthetized animals and fixed in 4 % PFA. At the chronic (30d) time point, animals were perfused transcardially with saline followed by 4 % PFA, post fixed in 4 % PFA and then transferred to a 0.01 % sodium azide in PBS solution. All gut segments were later embedded in cryo-OCT compound for cryostat sectioning. Cryosections (10 μm) were collected on glass slides (3 per slide) and analyzed for hematoxylin and eosin (H&E) staining, Periodic acid-Schiff and tomato lectin staining as previously described (Bake et al., 2019; Kumar, 2017). Sections were imaged with the Olympus

VS120 virtual slide scanning system.

4.5.1. Analysis of H&E staining

The villus length to villus width ratio was assessed for every villus on three sections per animal using the ImageJ software. The length of the villus was measured from its base at the crypt to its tip and its width was measured at its widest point. The number of crypts at the base of each villus was also counted.

4.5.2. Periodic acid-Schiff (PAS) stain

Cryosections were collected on glass slides and washed and fixed prior to PAS staining protocol (Sigma-Aldrich, 395B) using our established procedures (El-Hakim, 2021). Slides were air-dried and cover slipped using DPX media. Sections were imaged on the Olympus VS120 virtual slide scanning system. The number of goblet cells was counted for each villus on 3 sections per animal. Goblet cells were identified by their characteristic shape, pink coloration and location along the borders of the villi.

4.6. Lectin histochemistry

A lectin stain was performed on gut sections from animals terminated at 30d post stroke. Gut sections were fixed in 4 % PFA then washed in PBS and incubated with blocking buffer for 1 hr. Slides were then incubated with Lectin (1:1000, Vector Laboratories, CA) for 1 hr, washed with PBS and coverslipped with mounting media containing the nuclear dye DAPI (Fluoroshield, Abcam). Adjacent sections from each animal were coverslipped after the blocking step ('negative' or 'blocking control') to assess autofluorescence. All sections were then visualized and photographed on the FV3000 confocal microscope. Images were matched for exposure and contrast and analyzed for Mean Fluorescence Intensity (MFI) using ImageJ software. MFI of the blocking control was subtracted from the MFI of lectin-stained sections for each animal (normalized MFI). The normalized MFI was then subject to one way ANOVA to assess group differences.

4.6.1. Gut permeability analysis

Gut permeability test was performed at 2d post stroke as described in our previous published protocol (Bake et al., 2017; Kulesh et al., 2018). Size-graded dextrans labeled with either fluorescein isothiocynate (FITC, 10 kDa) or rhodamine (RhoD, 70 kDa) were administered by oral gavage (60 mg/ 100 g of body weight) to Sham, Vehicle or IP-IGF1 treated animals (n = 4 in all groups). All rats received the oral gavage at 2 days post-stroke, and blood was collected from the tail tip at 60, 90, and 120 min later. Blood samples were stored in the dark at 4∘C for 4 h, then centrifuged for 2 min at 1200 rpm and the supernatant was diluted into 1:1000-fold with 1xPBS. Prepared samples were added to a 96-well microplate to determine the concentration of fluorescently labeled dextran in the serum by spectrophotometer (Tecan, USA) with an excitation frequency of 490 nm and emission of 520 nm for FITCD-10 kDa, and excitation frequency of 540 nm and an emission of 625 nm for RhoD-70 kDa. Each assay plate also had known quantities of serially diluted FITC-dextran and Rho-dextran (5, 10, 100, 200, 300, 400, 500 and 600 ng/ml) standards. The plasma from a naive rat (not administered with labeled dextran) was used to determine the background.

5. Fecal metagenomics analyses

5.1. Boostershot® shallow shotgun metagenomic sequencing

The microbial DNA from fecal samples obtained at 30d after stroke was extracted and quantified using the MoBio PowerSoil® DNA isolation kit (MoBio Laboratories, Carlsbad, CA, USA) and the Quant-iT PicoGreen dsDNA assay kit (Thermo Fisher Scientific Inc., Waltham, MA, USA), respectively. For sequencing libraries preparation, the Nextera XT DNA Library Preparation Kit (Illumina Inc., San Diego, CA, USA) was used before the libraries were pooled. After this step, SPRI bead purification and concentration were processed using SpeedBeads Magnetic Carboxylate Modified Particles (Cytiva Life Sciences, Marlborough, MA, USA). The resulting pooled libraries were denatured by NaOH before being diluted and spiked by 2 % PhiX.

The metagenomic sequencing was performed on an Illumina NovaSeq 6000 System using a single-end 1x100 base pair read chemistry), followed by being multiplexed on the sequencer before converting to FASTQ files and filtering for low quality (Q-score < 30) and length (<50). Adapter sequences were trimmed, and all sequences were trimmed to a maximum length of 100 bp before alignment. The raw sequences were made using NCBI Sequence Read Archive before analysis with established pipelines. In terms of taxonomic classification, FASTA sequences were aligned making a curated database, which contained all representative genomes in the NCBI RefSeq, a representative genome collection for prokaryotes with additional manually curated strains for bacteria (O'Leary et al., 2016). Alignments were made at 97 % identity and compared to reference genomes. Every input sequence was compared to every reference sequence in the Diversigen DivDB-Dog database using fully gapped alignment with BURST. Ties were broken by minimizing the overall number of unique Operational Taxonomic Units (OTUs). The input sequences were listed as the lowest common ancestor for taxonomy assignment, which was compatible with not < 80 % of the reference sequences. OTUs accounting for less than one million of all species-level markers and OTUs with < 0.01 % of their unique genome regions matching as well as < 0.1 % of the whole genome were discarded.

For downstream analysis, normalized and filtered tables were used in QIIME2 (Bolyen et al., 2019). Kyoto Encyclopedia of Genes and Genomes (KEGG) orthology (KO) groups were observed with alignment at 97 % identity against a gene database derived from the NCBI RefSeq representative genome collection for prokaryotes with additional manually curated strains for bacteria mentioned above for functionally annotated genes (Kanehisa et al., 2010; Kanehisa et al., 2016). The directly observed KO counts reported as relative abundance within each sample were expressed in a KO table and downstream tables. Kos were then collapsed to level-2 and level-3 KEGG pathways and KEGG modules.

For this study, group differences in phyla abundance and selected species of the Lactobacillus genera was determined by ANOVA.

Abundance of Kegg modules from MCA0 + Vehicle and MCAo + IP IGF1 were compared by t-tests (corrected for FDR) and depicted by volcano plot and heat map. Groups were also subject to Principal Component Analysis to assess qualitatively the extent of overlap in the 2 groups. A similar analysis was also performed for MCA0 + Vehicle and MCAo + ICV-IGF1 groups.

5.2. Short chain fatty acid analysis

The following short-chain fatty acids (SCFAs) were analyzed in serum samples obtained post-stroke and in fecal samples: butyric acid, isobutyric acid, valeric acid, isovaleric acid, and propionic acid levels. Serum samples were aliquoted (50 ul) and extracted with a methanol: chloroform:water-based extraction method. In the cases of stool samples, 50 mg of lyophilized feces was extracted with ethyl acetate and absolute levels of fecal SCFAs were normalized to dried fecal weights. Both types of samples were spiked with 0.1 mM d7 butyric acid as an internal standard. SCFAs were detected and quantified on a gas chromatography triple quadrupole mass spectrometer (TSQ EVO 8000, Thermo Scientific, Waltham, MA) at the Texas A&M University Integrated Metabolomics Analysis Core.

6. Predictive modeling of stroke outcomes

Linear regression models were applied to conduct statistical inference; whether cognitive impairment could be associated with gut

microbes or metabolites in the IP-IGF1 study. Two measures of cognitive impairment were used as the response variable: Barnes latency Day 3 as a measure of learning ability and Barnes probe trial as a measure of recall. The explanatory variables considered were the numeric microbial phyla Firmicutes and Bacteroidetes, Lactobacillus species, and metabolite variables butyric acid, acetate, LPS. The form of the linear regression models was as follows:

Barnes latency (or probe trial) $= \beta 0 + \beta 1$ *Firmicutes* $+ \beta 2$ *Bacteroidetes* $+ \beta 3$ *Lactobacillus* $+ \beta 4$ *LPS*$+\beta 5$ *Butyrate* $+ \beta 6$ *Acetate.*

Here, β0 is the model intercept, β1,β2,⋯,β6 coefficients are the mean differences in Barnes latency (or probe trial) associated with one-unit increases in the metabolite variables while holding all other explanatory variables constant.

All models were fit using least squares. Model estimates, confidence intervals, and p values were computed under the standard least-squares regression assumptions. Statistical confidence was set at 95 %.

6.1. Statistical analyses

Data were primarily analyzed using parametric statistical tests (Prism Graphpad). Survival plots were calculated using the Kaplan Meier test. For behavioral tests, pre- and post-stroke scores were compared by a paired Student's *t* test. For all other comparisons, an unpaired Student's *t* test or a two-way ANOVA were used. Group differences were considered significant at $p < 0.05$ in each case. All data are expressed as mean ± S.E.M. Specific animal numbers used for an assay is described in each figure legend.

7. Results

7.1. Effect of ICV-IGF1 on acute stroke outcomes

Middle-aged (12 month old) female Sprague Dawley rats were assigned to the study once they were confirmed to be acyclic by daily vaginal smears. Animals were subjected to either MCAo or sham operation after establishing a baseline for the following tests: sensory motor performance, social interaction and novel object recognition test (NORT). Four hours after MCAo, rats received either vehicle or IGF1 by ICV (ICV-IGF1) infusion for 48-hours, while sham rats received vehicle infusions. All animals were terminated 2 days post stroke/sham surgery. ICV-IGF1 treated rats had a better survival rate (77.78 %) compared to the vehicle-treated rats (57.14 %), although this was not statistically significant (Fig. 1A, $p = 0.2817$). Representative images of coronal sections stained with TTC showed that vehicle-treated rats had qualitatively larger infarcts (Fig. 1B) as compared to ICV-IGF1 treated animals. When quantified, IGF1 treatment resulted in a 60 % decrease ($p < 0.0063$) of the infarct volume compared to vehicle treated animals (Fig. 1C). The acute neuroprotection observed in infarct volume was also reflected in better performance on sensory motor behaviors. In the adhesive tape removal test, latency to remove the tape was affected by stroke ($F_{(2,36)}$: 60.08, $p < 0.0001$) and by treatment ($F_{(2,36)}$: 23.69, $p < 0.0001$). MCAo resulted in longer latencies for tape removal at 2d and 5d post stroke. However, ICV-IGF1 treated animals had significantly shorter latencies at both time points as compared to vehicle treatment (Fig. 1D). A similar effect of stroke ($F_{(2,91)}$: 56.43, $p < 0.0001$) and treatment ($F_{(2,91)}$: 33.45, $p < 0.0001$) was seen in the 'same side' vibrissae evoked forelimb placement task. Vehicle-treated rats showed a significant deficit in paw placement reflex of the contralesional paw at 2 days and 5 days post stroke while IGF1 treated rats were no different from their baseline (pre-stroke) performance (Fig. 1E). In the cross-midline version of the task, both stroke ($F_{(2,36)}$: 40.78, $p < 0.0001$) and treatment ($F_{(2,55)}$: 61.74, $p < 0.0001$) affected the performance on this test. Both vehicle and IGF1-treated rats had a deficit at 2 days post stroke, however, by 5 days post stroke, the IGF1 treated rats had recovered but the vehicle-treated rats remained significantly impaired compared to pre-stroke performance (Fig. 1F). Collectively, these data indicate robust neuroprotection resulting from ICV-IGF1 delivery in the acute phase of stroke.

7.2. Effect of ICV-IGF1 on cognitive and affective behaviors in the chronic phase of stroke

A separate group of animals was prepared to assess the effect of the ICV delivery of IGF1 on long-term stroke outcomes including affective and cognitive function at 30 days post MCAo or sham surgery. All surgical and treatment protocols were similar to the acute studies.

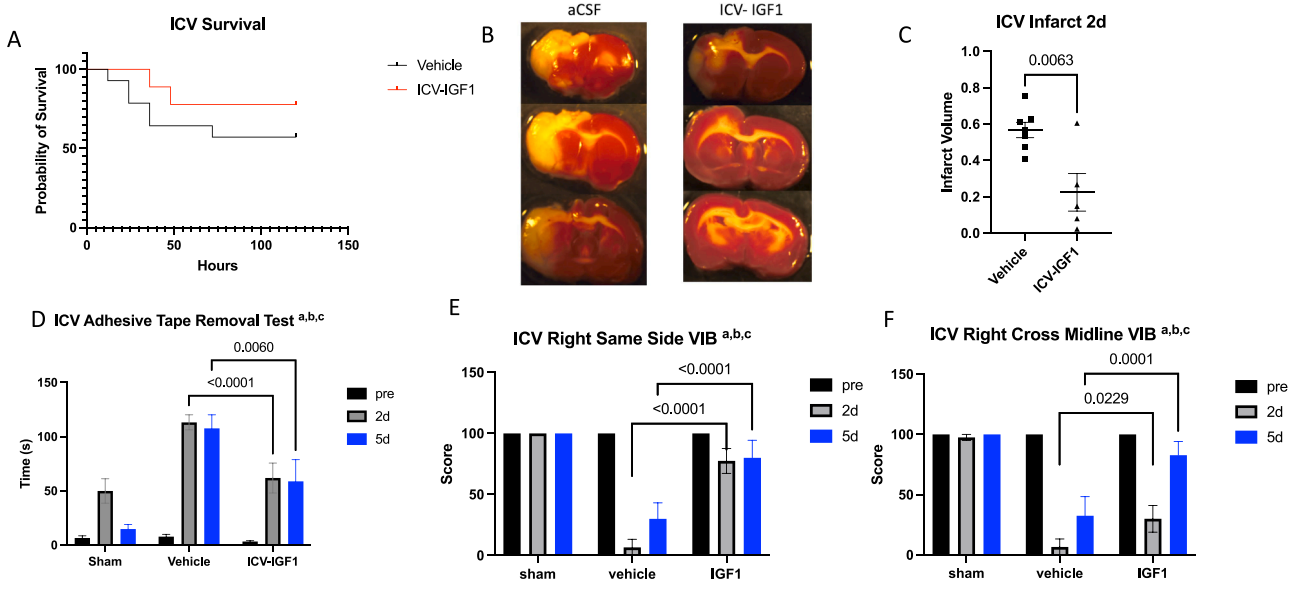

Fig. 1. *Effect of ICV-IGF1 on acute stroke outcomes.* A) Kaplan Meier survival plot depicting mortality after MCAo in vehicle-treated and ICV-IGF1 treated rats ($p = 0.2817$). B) Representative images of TTC-stained coronal sections from vehicle and ICV-IGF1 treated animals. C) Quantitation of infarct volume from TTC-stained sections. Sensory motor function was assessed by the (D) Adhesive Removal test (ART) and the (E) same side and (F) cross midline VIB test, pre stroke, 2d and 5d after stroke. Key [a]: main effect of stroke, [b]: main effect of treatment, [c]: interaction effect. n = 5–7/group. Exact p values for planned comparison as indicated in graphs.

7.3. Cognitive function was assessed by Barnes maze and NORT

Barnes maze test assesses learning and recall of a spatial task. Learning is determined by the latency to find the escape chamber, over 3 consecutive learning days, which typically decreases over this training period. Only sham rats showed effective learning as indicated by a significant difference between latencies on day 1 of learning and day 3 of learning, ($p = 0.0414$). This was not the case in the vehicle treated group ($p = 0.1865$) or the ICV-IGF1 treated group ($p = 0.3474$) (Fig. 2A). Velocity, or the speed at which animals locate the escape hole increased over time (main effect of time ($F_{(2,35)}$:11.47; $p = 0.0001$), however, there were no group differences in velocity, indicating that group differences seen in latency is likely due to difference in learning and not impaired motor ability (Fig. 2B). Learning was also assessed by the number of 'failed' trials, defined as failure to find the escape hole in the maximum allotted time for the trial (120 s). The percent of failed trails was assessed over the learning days and day 1 and day 3 of learning were again compared. None of the groups had decreased failures between day 1 and day 3 (sham $p = 0.3470$; vehicle $p = 0.6376$; ICV-IGF1 $p = 0.7512$) (Fig. 2C).

Cognitive function was further assessed for recall using the Barnes probe trial and by NORT. In the Barnes probe trial, which takes place two days after the last learning day, the goal box is replaced with a shallow box (like the rest of the maze) and the time spent in the quadrant where the goal box was originally located during the learning days is documented. There was no difference in the amount of time spent in the target quadrant between the vehicle and ICV-IGF1 treated groups ($p = 0.5773$) (Fig. 2D). In NORT, preference for a novel object over a familiar object, measured by the amount of time spent exploring the object, was assessed pre and 30 days post MCAo or sham surgery (Fig. 2E). Increased time spent exploring the novel object indicates retention of the memory of the familiar object and thus the ability to discriminate between the two objects (Panta, 2020). Preference was determined by the discrimination index (DI), where a positive number indicates a preference for the novel object. Only those animals that showed a preference for the novel object (positive non-zero DI) prior to stroke were included in this analysis. Overall, there was a stroke-related decrease in the exploration of the novel object (main effect of stroke; $F_{(1,16)}$: 4.623, $p = 0.0472$) where the vehicle and ICV-IGF1-treated MCAo rats had significantly lower DI scores post as compared to pre MCAo.

Affective behavior was assessed by the social interaction (SI) test. The test takes advantage of species natural behavior and is inherently rewarding to rodents. Thus less time spent in the 'social' chamber with the conspecific rat would indicate a depressive phenotype. There was a significant main effect of stroke ($F_{(1,12)}$: 7.655, $p = 0.0171$) and treatment ($F_{(1,12)}$: 6.259, $p = 0.0278$). Planned comparisons indicate that while both the IGF1 and vehicle treatment groups spent less time in the social chamber after stroke, this decrease was significant in the IGF1 treated group (Fig. 2F).

Collectively, these results indicate that while ICV delivery of IGF1 was robustly neuroprotective in the acute phase, this neuroprotection did not result in an attenuation of post stroke cognitive or affective outcomes.

7.4. Effect of ICV-IGF1 on brain volumetric analyses

Long-term changes in brain atrophy were assessed by three measures: the volume of the ischemic and non-ischemic hemisphere, lateral ventricular volume of each hemisphere and the width of the corpus callosum at midline. As show in Fig. 3A, volume of the ischemic hemisphere was significantly reduced as compared to the non-ischemic hemisphere in both MCAo groups, while the Sham group had similar hemisphere volumes. Compared to the non-ischemic hemisphere, the volume of the ischemic hemisphere volume was reduced to 88 % in the

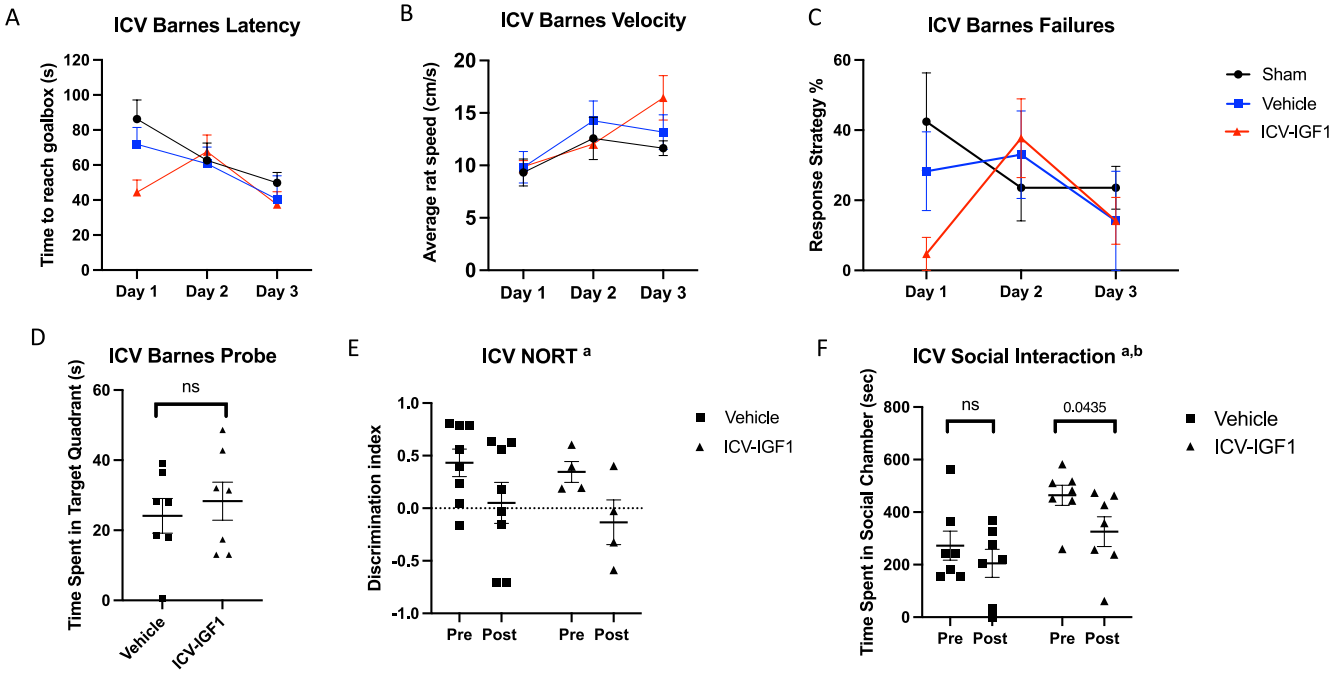

Fig. 2. *Effect of ICV-IGF1 on cognitive-affective behaviors in the chronic phase of stroke.* A) Latency to find the escape box was compared on training Day 1 with training Day 3 for each group. Sham $p = 0.0414$, vehicle-treated MCAo group $p = 0.1865$, ICV-IGF1 treated group $p = 0.3474$. B) Velocity to find the escape box over the learning days. C) Percent failures where the escape box was not detected over trials during the 3 training days. Comparison of failures on training Day 1 with training Day 3 for each group: Sham $p = 0.3470$; MCAo + vehicle: $p = 0.6376$; MCAo + ICV-IGF1: $p = 0.7512$. D) Recall of spatial memory assessed by the amount of time spent in the escape quadrant during the Barnes probe trial. MCAo + vehicle and MCAo + ICV-IGF1 groups: $p = 0.5773$). E) NORT discrimination index for preference of the novel object pre and post stroke. a: main effect of stroke. F) Social interaction task assessed by the amount of time spent in the social chamber pre- and post-stroke in vehicle and ICV-IGF1 treated animals. Key: [a]: main effect of stroke, [b] main effect of treatment. n = 6–8/group. Exact p values for planned comparison as indicated in graphs.

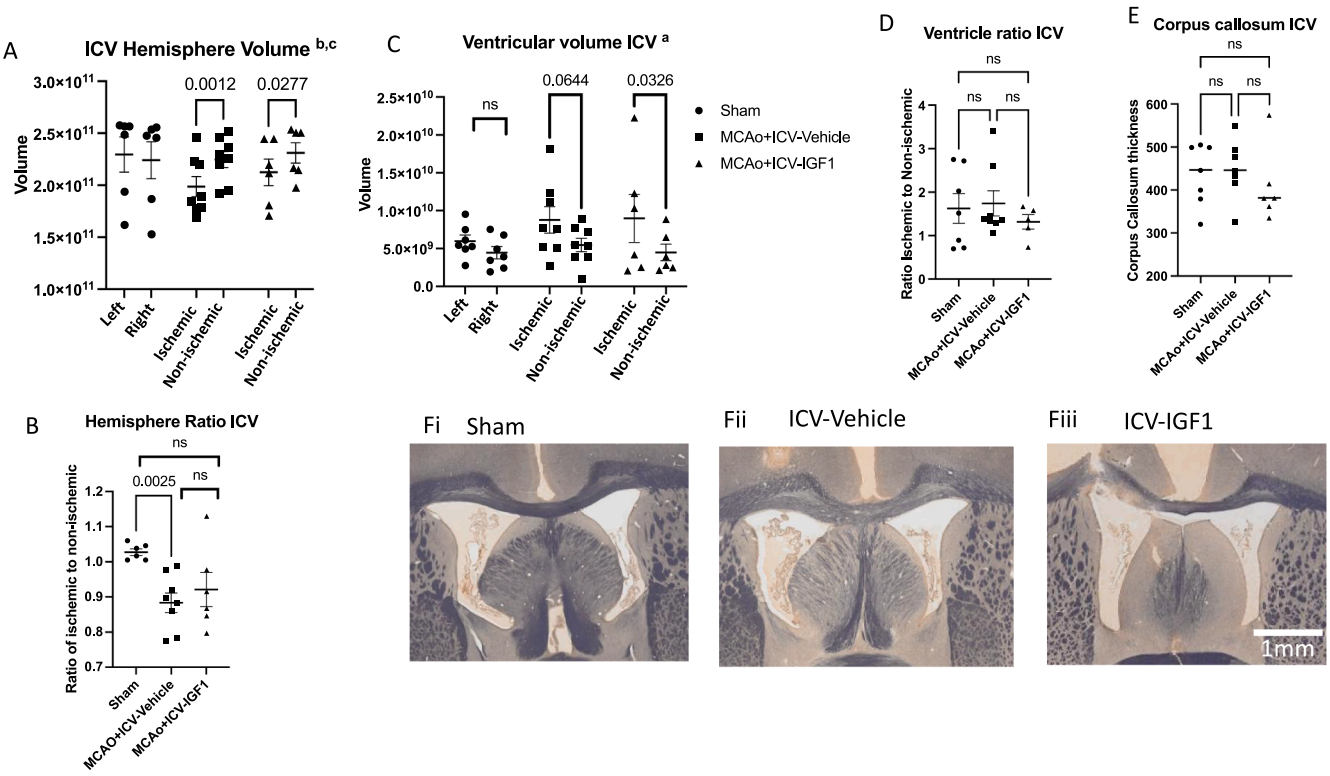

Fig. 3. *Effect of ICV-IGF1 on brain volumetric features in the chronic phase of stroke* (A) Volume of the ischemic and non-ischemic hemisphere and the (B) the volume of the ischemic hemisphere normalized to the non-ischemic hemisphere of Sham, MCAo + ICV-Vehicle and MCAo + ICV-IGF1 animals. (C) Lateral ventricular volume of the ischemic and non-ischemic hemisphere and the (D) the volume of the ventricular volume of the ischemic hemisphere normalized to the non-ischemic hemisphere of Sham, MCAo + ICV-Vehicle and MCAo + ICV-IGF1 animals. (E) Width of the corpus callosum at the midline in the Sham, MCAo + ICV-Vehicle and MCAo + ICV-IGF1 animals. (Fi-Fiii) Representative images of the Weil myelin-stained sections depicting the lateral ventricles and the corpus callosum from Sham, MCAo + ICV-Vehicle and MCAo + ICV-IGF1 animals. N=5–7 per group, paired *t*-test for A and C (Sidaks multiple comparison tests) and Dunnett's multiple comparison tests for B, D, E; exact p values are shown on the graph.

ICV-Vehicle treated group, and 92 % in the ICV-IGF1 groupM (Fig. 3A). This ratio was significantly different between the ICV-Vehicle compared to Sham, while the ratio was intermediate in the ICV-IGF1 group (not different from sham or ICV-Vehicle (Fig. 3B). Ventricular asymmetry which is indicative of atrophy was also seen in ICV-Vehicle and ICV-IGF1 groups (Fig. 3C), however, no group differences were noted in the ratio of left and right ventricular volume (Fig. 3D). Similarly, no group differences were seen in the width of the corpus callosum between the three groups (Fig. 3E). It should be noted that this group had an in-dwelling cannula in the ventricle (for ICV drug delivery), thus some distortion of the ventricle may obscure stroke related effects. Representative images of the later ventricle and midline corpus callosum are shown in Fig. 3Fi-iii.

7.5. Effect of IP-IGF1 on acute stroke outcomes

To determine whether peripheral administration of IGF1 would result in a better acute and chronic outcome after stroke, a separate cohort of animals was prepared where rats were given either a vehicle or IGF1 IP injection at 4 h and 24 h post stroke. Recombinant human IGF1 (rhIGF1) levels were measured in serum by ELISA (assay range 0.1–4 ng/ml) and showed that IGF1 treated rats had 0.824 ng/ml of hrIGF-1 in plasma, while hrIGF-1 was virtually undetectable in sham (0.055 ng/ml) and vehicle (0.06 ng/ml) animals. In the brain (cortex and striatum), rhIGF1 was completely undetected (below detection limit of the assay). The animals were terminated at the 2-day or 5-day after MCAo to examine the effect of the IP-IGF1 treatment on acute stroke outcomes by the same metrics as the ICV treatment (described above). IP-IGF1 treatment was not neuroprotective in the acute phase of stroke. Survival was similar in the IP-IGF1 group (69.5 %) to the vehicle group (62.5 %) (Fig. 4A). Infarct volume was no different between the IP-IGF1 and vehicle groups at 2 days post MCAo ($p = 0.4968$), and 5d post stroke ($p = 0.5817$) (Fig. 4B and C). Additionally, in the sensory motor tests, stroke-induced deficits were observed in the adhesive tape removal and the same side and cross midline vibrissae evoked forelimb placement tasks in both the vehicle and IP-IGF1-treated rats, however, no difference was observed between these two treatment groups (Fig. 4D–F). In the cross midline VIB task, both IGF1 and vehicle groups had a partial recovery at the 5d time point as compared to the 2d time point. Collectively, these results indicate that the IP route of administration did not result in neuroprotection in the acute phase of stroke, indicating that local availability of IGF1 at the ischemic site (ICV-IGF1) is critical for

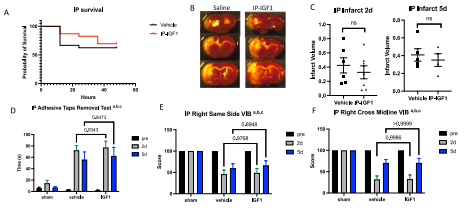

Fig. 4. *Effect of IP-IGF1 on acute stroke outcomes.* A) Kaplan Meier survival plot depicting mortality after MCAo in vehicle-treated rats and IP-IGF1 treated rats ($p = 0.5210$). B) Representative TTC-stained coronal slices from vehicle and IP-IGF1 treated animals. C) Quantification of infarct volume from TTC-stained sections at 2d ($p = 0.4968$) or 5d ($p = 0.5817$) post stroke. Sensory motor function was assessed by the (D) Adhesive Removal test (ART) and the (E) same side and (F) cross midline VIB test, pre stroke, 2d and 5d after stroke. Key: [a] main effect of stroke, [b]: main effect of treatment, [c]: interaction effect. n = 5–7/group. Exact p values for planned comparison as indicated in graphs.

neuroprotection.

7.6. Effect of IP-IGF1 on post-stroke changes in affect and cognition

To assess the effect of the IP route of administration on long-term behavior outcomes, a separate cohort of rats was prepared, and given the same treatment regimen and subjected to the same behavior tests as previously described.

Barnes maze: Over the 3-day training period, there was an overall decrease in the latency to find the escape box. However, this decreased latency was significant in the sham group (day 1 vs day 3, $p = 0.0198$) and IP-IGF1 treated stroke group (day 1 vs day 3, $p = 0.0112$), but not in the vehicle-treated stroke animals (day 1 vs day 3, $p = 0.3184$) (Fig. 5A). As shown in Fig. 4B, while velocity improved over the three day period (main effect of time $F_{(2,44)}$: 8.79, $p = 0o.0006$) no group differences were noted in velocity, indicating that motor performance was similar in all groups, and that group differences in latency are likely due to differences in learning strategy. This is supported by our analysis of 'failed' trials over the 3 learning days. Comparing the number of failures between day 1 and day 3 of learning, both the Sham ($p = 0.0197$) and IP-IGF1 treated MCAo rats ($p = 0.0410$), had a significant decrease in failures, while the vehicle-treated MCAo rats did not ($p = 0.8035$) (Fig. 5C).

Recall, another aspect of cognition, was measured on the probe trial of Barnes maze task and NORT. The Barnes maze probe trial occurred 2d after the last learning day. The longer time the animal spends in the target quadrant (where the escape hole was previously located) is indicative of better recall. In the 1 min probe trial, IP-IGF1 treated animals spent a significantly longer time ($p = 0.0327$) in the target quadrant (30.0 +/-2.89 sec) than the vehicle group (18.42 +/- 3.939 secs) (Fig. 5D).

Episodic memory was tested in the NORT, where the ability to discriminate the novel object is indicated by a positive discrimination score. Only those animals that showed a preference for the novel object in the pre stroke test are included in this analysis (positive non-zero DI). There was a main effect of stroke ($F_{(1,9)}$: 14.14, $p = 0.0045$), such that the DI was lower after stroke. However, planned comparisons showed that this effect was largely driven by the vehicle-treated group (Fig. 7E). As compared to their pre stroke values, the vehicle group showed a significant lack of preference for the novel object as indicated by the decreased DI score ($p = 0.0136$) whereas the DI score of the IP-IGF1 group was not significantly different after stroke (Fig. 5E).

Similar to the ICV study, stroke had a significant effect on social interaction ($F_{(1,29)}$: 14.19, $p = 0.0008$), resulting in a general decreased interaction with the conspecific irrespective of icv-IGF1 treatment (Fig. 5F).

Taken together, these results indicate that the IP route of administration of IGF1 attenuated stroke-induced cognitive impairment.

7.7. Effect of IP-IGF1 on brain volumetric analyses

Long-term changes in brain atrophy were assessed by three measures (as above): the volume of the ischemic and non-ischemic hemisphere, lateral ventricular volume of each hemisphere and the width of the corpus callosum at midline. As show in Fig. 6A, volume of the ischemic hemisphere was not significantly different compared to the non-ischemic hemisphere in both MCAo groups, or the Sham group. Compared to the non-ischemic hemisphere, the volume of the ischemic hemisphere volume was reduced to 95 % in the IP-Vehicle treated group, and 96 % in the IP-IGF1 group (Fig. 6A). This ratio was significantly different between the MCAo + IP-Vehicle compared to Sham, and IP-IGF1 compared to sham (Fig. 6B), indicating a small but significant shrinkage of the ischemic hemisphere due to stroke. Ventricular enlargement which is also indicative of atrophy was seen in IP-Vehicle but not the IP-IGF1 group (or Sham) (Fig. 6C). A ratio of the left and right ventricular volume was significantly elevated in IP-Vehicle group compared to Sham (Fig. 3D), but not between the IP-IGF1 and Sham. The width of the corpus callosum was significantly reduced in the IP-Vehicle group compared to either Sham or IP-IGF1 groups, indicating a stroke-induced volumetric reduction of a major myelinated pathway that was attenuated by IP-IGF1 (Fig. 6E). Representative images of the later ventricle and midline corpus callosum are shown in Fig. 6Fi-iii.

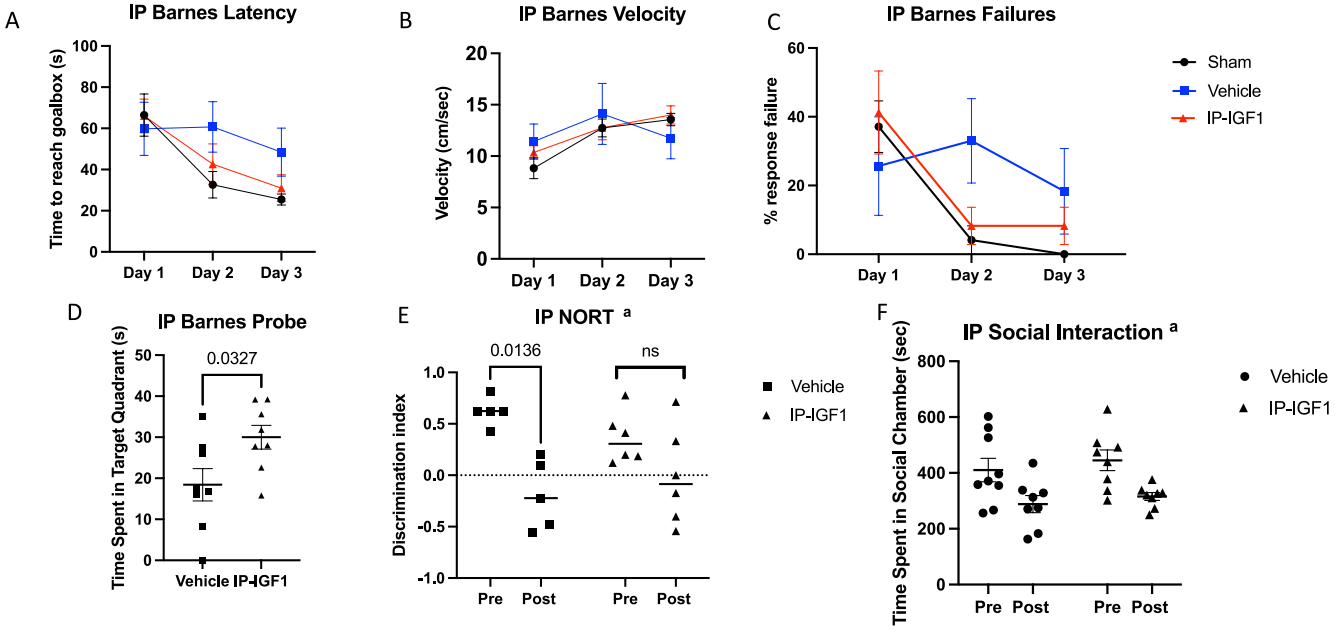

Fig. 5. *Effect of IP-IGF1 on cognitive and affective behaviors in the chronic phase of stroke.* A) Mean latency to find the escape box in Sham, MCAo + vehicle, MCAo + IP-IGF1 groups. Latency on training Day 1 compared with training Day 3 for each group: Sham $p = 0.0198$, MCAo + vehicle group $p = 0.3184$, MCAo + IP-IGF1 group $p = 0.0112$. B) Velocity to find the escape box over the learning days. C) Failures in task completion over the 3 training days. Sham $p = 0.0197$; vehicle treated MCAo rats $p = 0.8035$ and IP-IGF1 treated MCAo rats $p = 0.0410$. D) Time in the target quadrant of the Barnes probe trial (*: $p = 0.0327$). E) NORT task: a: effect of stroke, with planned comparisons pre and post stroke for MCAo + vehicle treated group and MCAo + IP-IGF1. F) Social interaction: histogram shows time spent in the social chamber pre and post-MCAo. a: main effect of stroke. n = 6–9/group. Exact p values for planned comparison as indicated in graphs.

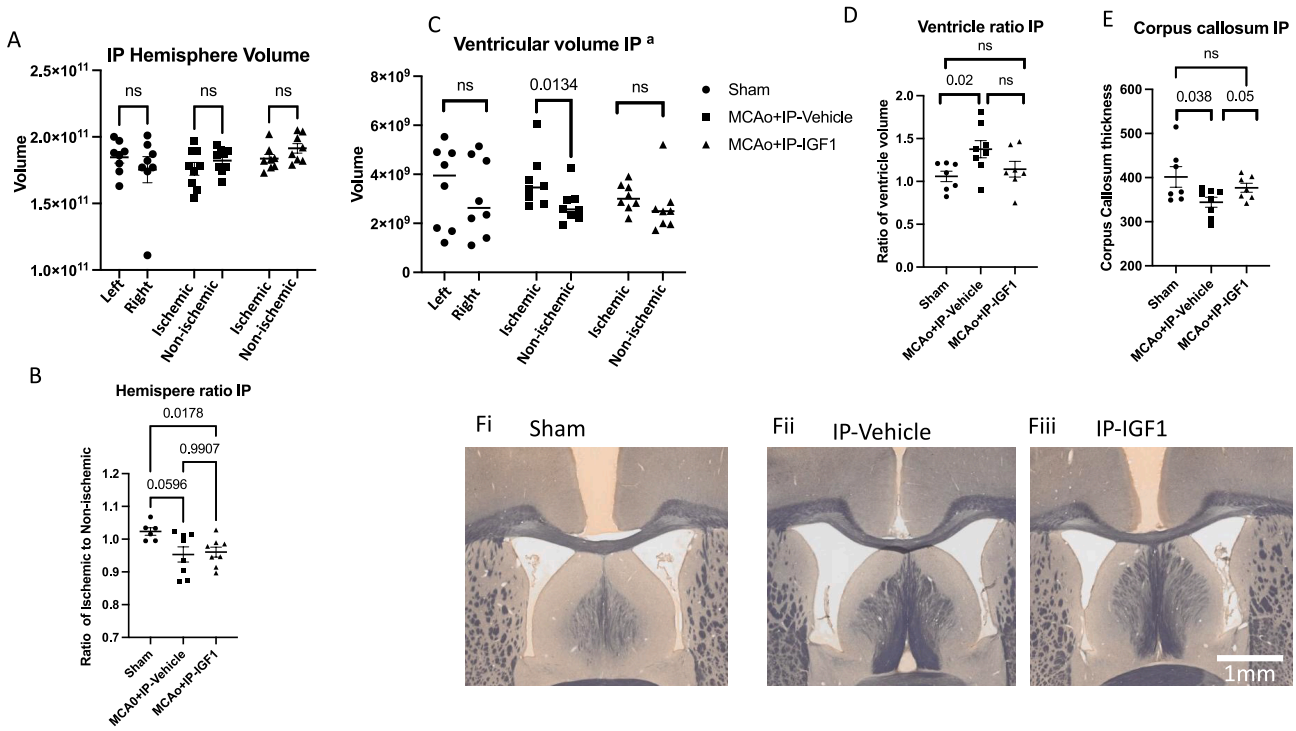

Fig. 6. *Effect of IP-IGF1 on brain volumetric features in the chronic phase of stroke* (A) Volume of the ischemic and non-ischemic hemisphere and the (B) the volume of the ischemic hemisphere normalized to the non-ischemic hemisphere of Sham, MCAo + IP-Vehicle and MCAo + IP-IGF1 animals. (C) Lateral ventricular volume of the ischemic and non-ischemic hemisphere and the (D) the volume of the ventricular volume of the ischemic hemisphere normalized to the non-ischemic hemisphere of Sham, MCAo + IP-Vehicle and MCAo + P-IGF1 animals. (E) Width of the corpus callosum at the midline in the Sham, IP-Vehicle and IP-IGF1. (Fi-Fiii) Representative images of the Weil myelin-stained sections depicting the lateral ventricles and the corpus callosum from Sham, MCAo + IP-Vehicle and MCAo + P-IGF1. N=6–8 per group, paired *t*-test for A and C (Sidak's multiple comparison tests) and Dunnett's multiple comparison tests for B, D, E; exact p values are shown on the graph.

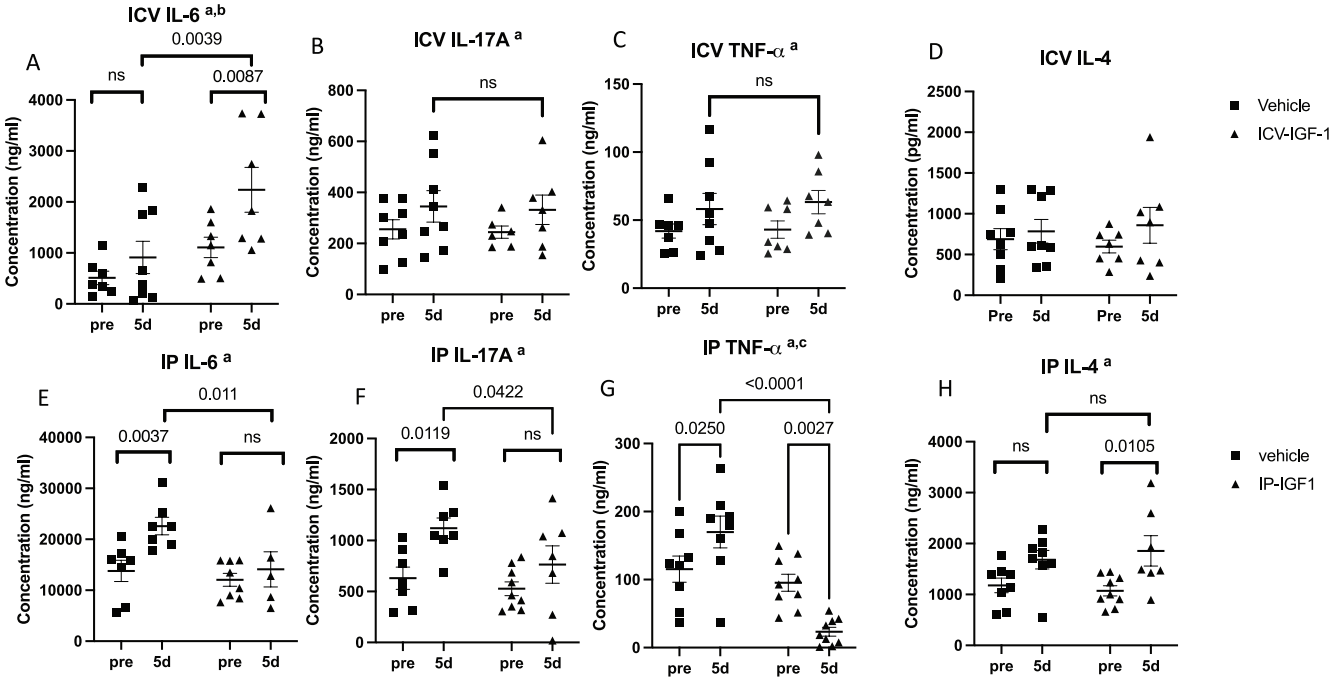

Fig. 7. *Effect of ICV and IP IGF1 treatments on serum inflammatory cytokines in the acute phase of stroke.* Histogram depicts levels of IL-6, IL17a, TNF-α, and IL4 in serum samples obtained pre and 5d post stroke from the ICV-IGF1 study (A-D) and the IP-IGF1 study (E-H). All cytokines were analyzed by 2 way ANOVA and planned comparisons. Key: [a]: main effect of stroke, [b]: main effect of treatment, [c]: interaction effect of stroke and treatment. n = 5–7/group. Exact p values for planned comparisons as indicated in graphs.

7.8. Effect of ICV and IP IGF1 treatments on serum inflammatory cytokines in the acute phase of stroke

In view of the evidence that peripheral inflammatory mediators are elevated in both depression and cognition, we examined the efficacy of the IGF1 treatment in attenuating stroke-induced increases in the pro-inflammatory cytokines IL-6, IL-17A and TNF-α and anti-inflammatory cytokine IL-4 in the acute phase. ICV-IGF1 failed to ameliorate long-term behavior deficits and as expected, also failed to attenuate stroke-related increase of proinflammatory cytokines IL-6, IL-17A and TNF-α when measured at 5d after MCAo. As shown in Fig. 7A–C, there were significant stroke-related increases in IL-6 (main effect of stroke, $F_{(1, 12)}$:8.719; p = 0.0121), IL-17A (main effect of stroke $F_{(1,12)}$: 4.842, p = 0.0481) and TNF-α($F_{(1,25)}$: 4.503, p = 0.0439). While the stroke-induced increase in IL-17A and TNF-α was similar in MCAo + Vehicle and MCAo + ICV-IGF1 groups, the ICV-IGF1 treated group had higher levels IL-6 as compared to vehicle-treated animals (p = 0.0039) at 5d post stroke. IL-4 was not regulated in the ICV study by stroke (p = 0.5640) or by treatment (IL-4, p = 0.9567) (Fig. 7D). The lack of effect of ICV-IGF1 on these inflammatory cytokines is consistent with its ineffective impact on cognitive function. One possibility is that while IGF1 is shown to have an anti-inflammatory effect locally (Bake et al., 2014), the brain parenchymal delivery of IGF1 may have precluded its actions on peripheral immune cells/organs.

Similar to the ICV study, these cytokines were assayed pre and 5 days post stroke in the IP study as well. There was a main effect of stroke in the case of Il-6 and IL-17A, with vehicle-treated rats showing an approximate 2-fold increase in IL-6 (p = 0.0037) and IL-17A (p = 0.0119). IP-IGF1 treatment attenuated stroke-induced elevation in both cytokines, such that there were no differences between the pre and post stroke levels of these cytokines (IL-6: p = 0.7073; IL-17A: p = 0.3258). Additionally, levels of both IL-6 (p = 0.011) and IL-17A (p = 0,0422) were lower in the IP-IGF1 treated group as compared to the vehicle group after stroke (Fig. 7E and F). In the IP study, TNF-α showed a remarkable interaction effect of stroke and treatment, such that while TNFα levels were similar baseline, stroke elevated this cytokine in the vehicle group (p = 0.0250) but downregulated in the IP-IGF1 group (p = 0.0027) (Fig. 7G). Overall, this resulted in a 7-fold decline in TNF-α due to IP-IGF1 as compared to vehicle treatment (p < 0.0001). Relatedly, IL-4, an anti-inflammatory cytokine was elevated after stroke. While IL-4 was elevated by IP-IGF1 compared to its baseline (p = 0.0105), there was no significant difference in IL-4 levels in the vehicle and IP-IGF1 group after stroke (Fig. 7H). Taken together, these results indicate that IP-IGF1 treatment attenuates peripheral levels of pro-inflammatory cytokines and long-term behavior consequences, whereas the ICV route is ineffective in both, despite a profound neuroprotective effect in the acute phase.

7.9. Effect of ICV and IP IGF1 treatments on gut permeability

Two serum analytes, LPS and intestinal fatty acid binding protein (iFABP), were measured as surrogate markers for gut permeability, at 2d and 30 days post stroke. In both studies, LPS levels were elevated at 30d after stroke compared to the early acute (2d) time point. In the ICV study, the IGF1 treated MCAo group had higher serum levels of LPS than both sham (p = 0.007) and vehicle treated MCAo rats (p = 0.0045) (Fig. 8A). In contrast, in the IP study, LPS levels were elevated in the vehicle-treated MCAo group as compared to the sham rats (p = 0.006) while the IP-IGF1 group was not significantly different from sham (p = 0.2077) (Fig. 8B). Since serum LPS is indicative gut permeability and is known to impair the blood brain barrier, these results suggest a persistent gut disruption in the chronic phase of stroke and suggest a gut-protective effect of IP-IGF1 treatment that is not seen in the ICV-IGF1 treatment.

iFABP, a small protein synthesized by gut enterocytes, is released into circulation when enterocytes are damaged. In the ICV study, iFABP was increased in the MCA0 + vehicle group compared to the sham group (p = 0.0028). However, the ICV- IGF1 group was not significantly different from either the Sham (p = 0.2395) or the vehicle treated (p = 0.0927) group (Fig. 8C), suggesting an intermediate effectiveness of this treatment. In the IP study, plasma levels of iFABP were increased in the MCAo + vehicle group compared to sham (p = 0.0330; Fig. 8D). In

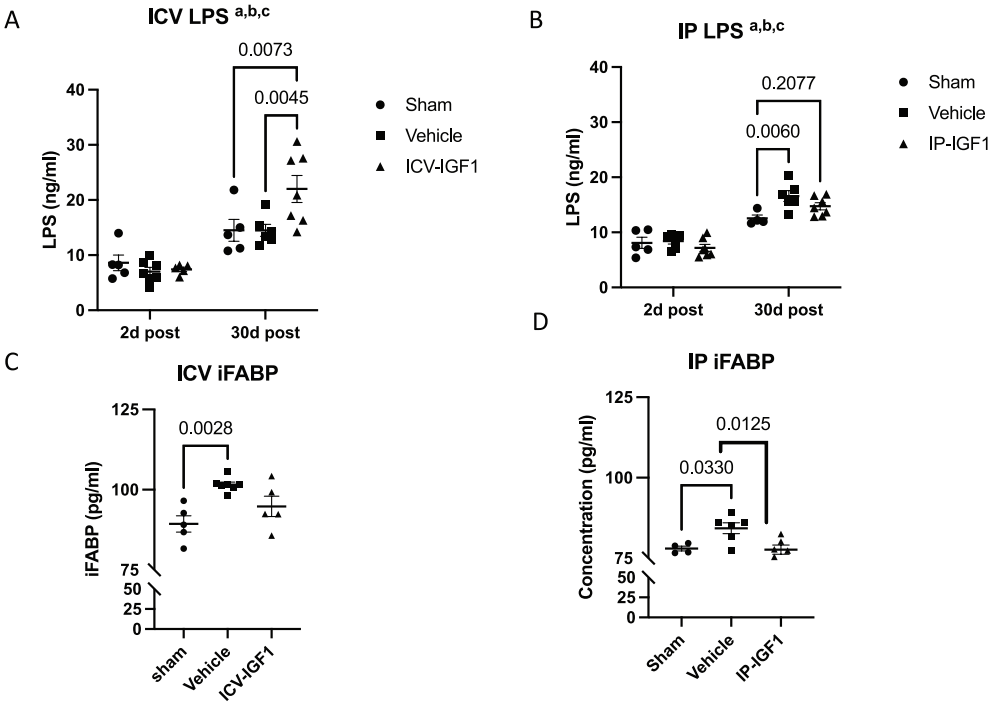

Fig. 8. *Analysis of surrogate markers of gut permeability*. Serum LPS and iFABP levels were measured to assess gut permeability. A) Serum LPS in the ICV study at 2d and 30 days post MCAo. B) Serum LPS levels in the IP study at 2d and 30 days post C) Serum iFABP levels in the ICV study at 2d post MCAo. D) Serum levels of iFABP in the IP study at 2d post MCAo. n = 5–8/group. Exact p values for planned comparison as indicated in graphs.

contrast, iFABP levels were lower in the MCAo + IP-IGF1 treated group (p = 0.0125) as compared to the vehicle-treated stroke group and was no different from the Sham group (Fig. 8D).

Both these analytes suggest that gut permeability is likely impacted by stroke and this pathology is attenuated in the IP-IGF1 treated animals. Gut permeability was further assessed in the IP-IGF1 group in the acute phase (2d post MCAo), using oral gavage of a 10kd and 70kd fluorescently labeled dextrans. In the case of the 10kD dextran, no group differences were seen due to either stroke or IGF treatment (Supplementary Figure 1A). In the case of the 70kD dextran, the MCAo + vehicle group showed elevated levels of this dextran compared to sham animals at 60 mins post gavage, while the MCAo + IP-IGF1 group was no different from the Sham or the MCA0 + Vehicle at this time point (Supplementary Figure 1B), partially supporting the conclusion that IP-IGF1 attenuates gut permeability.

7.10. Effect of IGF1 treatment on the gut after stroke

Our previous work shows there is an immediate and significant dysmorphology in the gut as a response to stroke which is associated with severe stroke outcomes (El-Hakim, 2021). In view of the data on inflammatory cytokines, cognitive impairment, surrogate markers of gut damage, as well as the ameliorative effect of IP-IGF1 treatment on these measures, we next tested the effect of IP-IGF1 on various aspects of gut histology.

7.11. Assessment of gut histology after MCAo and treatment with IP-IGF1

Coronal sections of the ileum stained for H&E showed that sham animals had evenly-spaced elongated villi and a single row of crypt cells. Sections from vehicle-treated stroke animals (MCAo + vehicle) show a characteristic pattern of gut dysmorphology including blunted and wide villi, and crypt hyperplasia (Fig. 9A). In the IP-IGF1 group, gut sections showed long tubular villi and a single row of crypt cells (Fig. 9A), similar to the sham animals.

Gut dysmorphology was quantified by two measures, crypt hyperplasia assessed by the number of crypts per villus and villus blunting assessed by the ratio of villus length to villus width. As shown in Fig. 9B, there was a 2-fold increase in the number of crypts per villus in the MCAo + IP-vehicle group as compared to the MCAo + IP-IGF1 (p = 0.0263) and sham (0.0394) groups. Similarly, the villus length to width ratio was decreased 2-fold in the MCAo + vehicle group which was significantly different from sham (p = 0.0166) and the MCAO+IP- IGF1 group (p = 0.0252) (Fig. 9B). Overall, the IP study indicated that MCAo resulted in gut dysmorphia which was attenuated by IP-IGF1 treatment.

At 30d post stroke, no obvious group differences are seen in gut morphology (Fig. 9C). In all cases, there appears to be a single row of crypt cells with tubular villi. While this is likely due to the normal regenerative processes where the gut cells turn over in a 4–5 day period, it is possible that there are subtle morphological features that remain altered even at this time.

Parallel analysis of gut sections from the ICV study (acute phase) showed that the Sham group had evenly sized, albeit blunted villi, while MCAo resulted in irregular shaped villi and significant crypt hyperplasia in both the vehicle and ICV-IGF1 treated groups (Supplementary Figure 2), Thus villus crypt morphology in the ICV-IGF1 group was consistent with elevated levels of LPS, a surrogate marker for gut permeability. All subsequent analysis of the gut was conducted on tissues from Sham, MCAo + Vehicle, and MCAo + IP-IGF1 groups.

7.12. Assessment of mucin barrier dysfunction

In addition to the villus-crypt histology, the mucin barrier is a critical component of also gut health. Period acid Schiff's (PAS) stain, which stains mucin and goblet cells, was performed on the ileum samples at the acute and chronic time points. At the acute time point, in sham animals, a continuous pattern of stain (pink) was observed on the borders of the villi, indicating a continuous and intact mucin barrier. Qualitatively, PAS staining was dysregulated in MCAo + vehicle group (Fig. 10A), possibly due to the changes in the villus morphology. In contrast, PAS staining was clearly visible in the intervillus space in the MCAo + IP-IGF1 group. Mucin-2 is a large protein (~350 kda) and its presence in blood circulation is indicative of profound damage to the gut-blood barrier. While there were no differences in the levels of Mucin-2 in Sham and MCAo + Vehicle groups, IP-IGF1 significantly decreased serum levels of mucin-2 (p = 0.0322) suggesting that IGF1 may act independently to exclude mucin-2 from circulation (Fig. 10B).

In the chronic phase, no qualitative differences were seen in distal ileum sections from the stroke and treatment groups (Fig. 10C). Goblet cells, the mucin-producing cells in the gut, were quantified per villus. Sham and MCAo + vehicle groups had similar numbers of goblet/villus, however, MCAo + IP-IGF1 group rats had significantly more goblet cells per villus than either the vehicle-treated MCAo rats or sham rats ($F_{(2,7)}$: 15.18, p = 0.0028) (Fig. 10D).

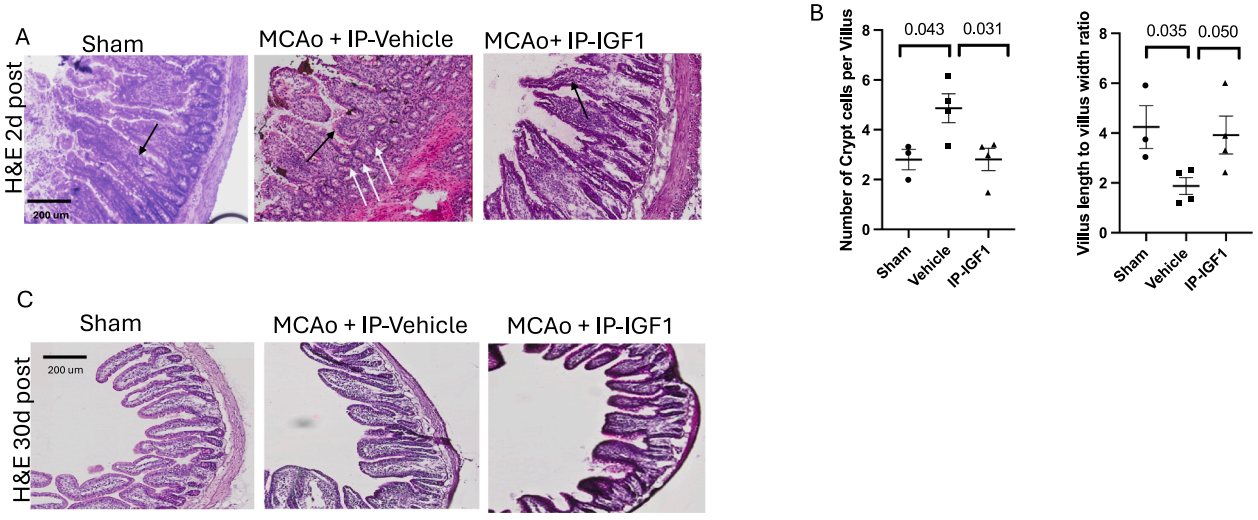

Fig. 9. *Assessment of Gut dysmorphia.* A) H&E-stained sections of ileum from IP study at 2d post MCAo. B) Villus length to width ratio and number of crypt cells per villus for the IP study. Exact p values for planned comparison as indicated in graphs. C) H&E-stained sections of ileum from IP study at 30d post MCAo. n = 3–5/group.

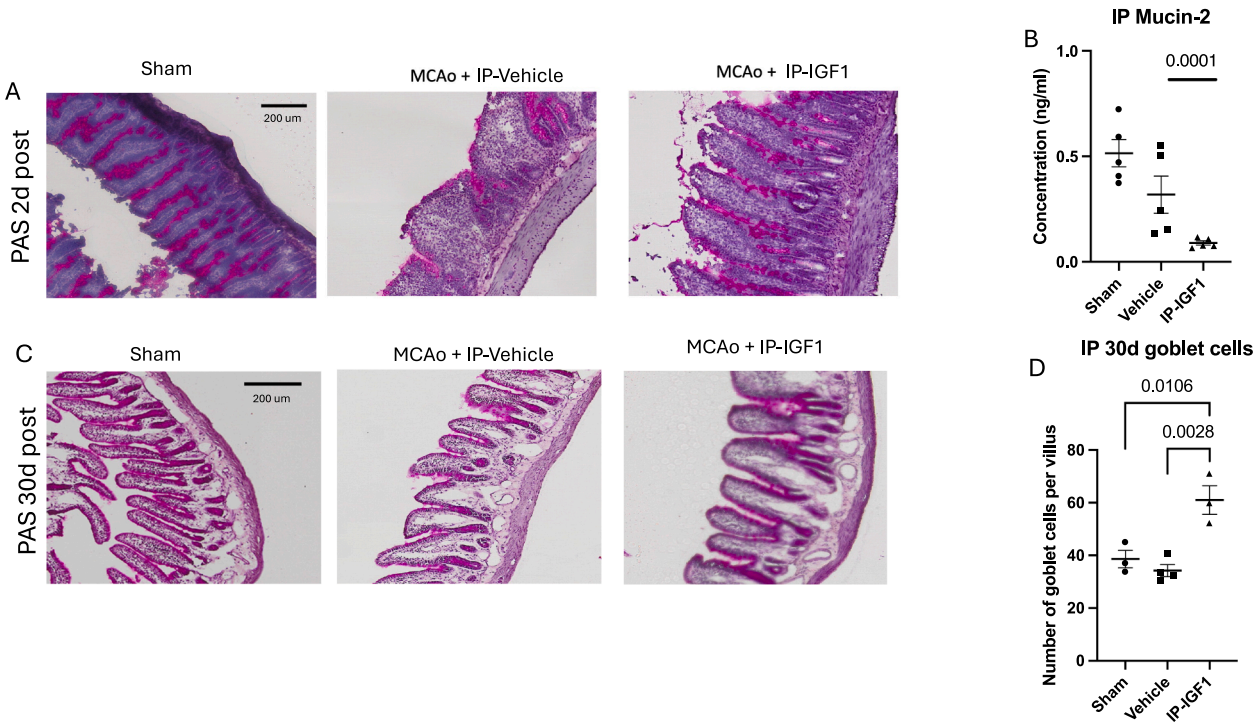

Fig. 10. *Assessment of mucin barrier dysfunction in IP study.* Photomicrographs of PAS-stained sections from sham, MCAo + vehicle and MCAo + IP-IGF1 at (A) 2d post and (C) 30d post MCAo. B) Serum mucin-2 levels in sham, MCAo + vehicle and MCAo + IP-IGF1 groups. D) Number of goblet cells per villus at 30d post MCAo. n = 3–5/group. Exact p values for planned comparison as indicated in graphs.

Taken together, these results indicate that the IP-IGF1 treatment had a reparative effect on the gut in the acute phase of stroke.

7.13. Effect of IP −IGF1 on gut vasculature

Since endothelial cells are a substrate for IGF1, a stain was performed on ileum sections to evaluate the effect of the IP treatment on the gut vasculature. Fluorescent lectin staining was seen in all groups to varying extents (Fig. 11A). Autofluorescence, assessed from blocking control sections, was low and no group differences were seen in auto-fluorescence. Analysis of variance of normalized MFI of lectin-stained sections confirmed qualitative differences in staining intensity ($F_{(2,10)}$: 4.616, p = 0.0380). Planned comparisons showed that vehicle-treated MCAo rats had decreased lectin fluorescence intensity as compared to sham (p = 0.0366), while IP-IGF1 treated animals were no different from sham (p = 0.6728), indicating that IP-IGF1 treatment rescued this effect of MCAo (Fig. 11B). IGF1 is known to promote growth of endothelial cells and microvessels, and the elevated levels of rhIGF1 in the serum of the IP treated rats is consistent with its beneficial effect on gut vasculature.

7.14. Assessment of gut dysbiosis and peripheral levels of SCFAs in the IP study

Gut permeability and dysmorphology may cause gut dysbiosis by allowing facultative anaerobes to bloom at the expense of obligate species. We previously reported gut permeability in the acute phase of stroke in adult animals (5–7 months of age) but did not detect changes in

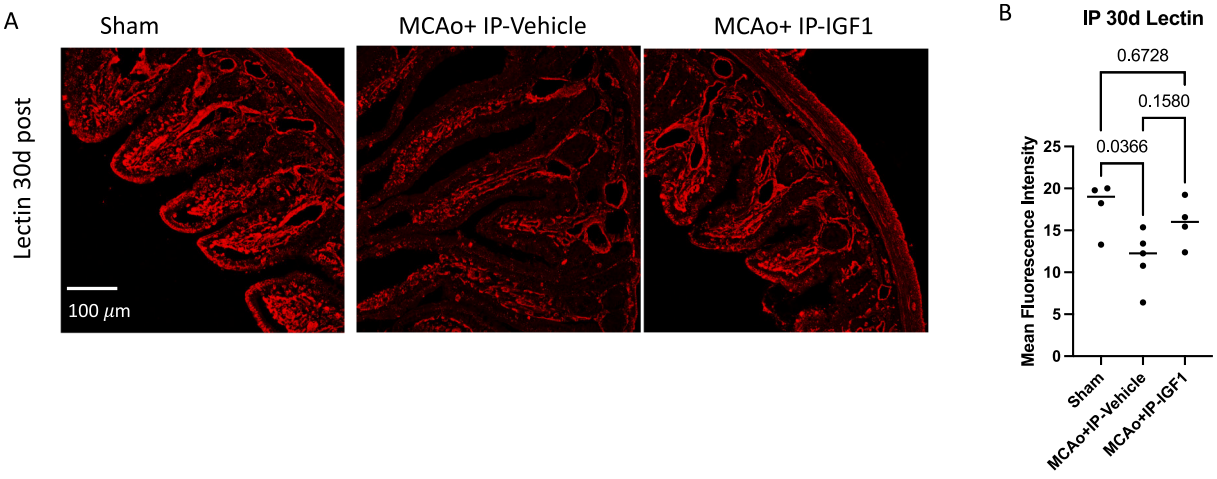

Fig. 11. *Assessment of gut vasculature in the IP study*. A) Lectin staining of ileum sections at 30d post MCAo. B) Mean fluorescence intensity analysis of lectin staining n = 4–5/group.

gut microbial communities at this time point (El-Hakim, 2021). Fecal samples obtained 30d after MCAo were subjected to shallow shotgun sequencing and the abundance of major phyla were analyzed. The two largest phyla, Bacteroidetes and Firmicutes, were altered by stroke and rescued by IP-IGF1 (Fig. 12A). Specifically, Firmicutes, the most abundant phyla, were decreased in vehicle-treated MCAo rats, to almost half of that seen in sham and IP-IGF1 treated MCAo rats. In contrast, Bacteroidetes were elevated almost 2-fold in the vehicle-treated MCAo group as compared to sham and IP-IGF1 MCAo rats.

This group difference in the abundance of major phyla was further reflected in modifications of bacterial gene expression. Comparison of KEGG Orthology pathways between MCAo + vehicle and MCAo + IP-IGF1 treated animals showed almost a third of these pathways were differentially expressed between the 2 groups. Principal component analysis and heat map arrays showed little overlap between the MCAo + vehicle and MCAo + IP-IGF1 groups. In contrast, only 1 % of the KO pathways differed between the vehicle and ICV-IGF1 treated groups and the groups showed significant overlap (Supplementary Figure 3).

A prominent genus in the Firmicutes phylum is Lactobacillus, consisting of several bacterial species with significant neuroprotective (Ma, 2019; Song, 2022) properties. Abundance of well-known lactobacillus species (including gasseri, johnsonii, reuteri, taiwanensis, murensis) is significantly reduced in the MCAo + vehicle group ($F_{(2,13)}$: 4.964, p = 0.0250) as compared to sham (p = 0.0504) and IP-IGF1 treated (p = 0.0231) rats (Fig. 12B).

Short chain fatty acids are a significant category of gut metabolites capable of modifying inflammation. Acetate is the main product of the Bacteroidetes phylum while butyrate is mainly produced by the Firmicutes phylum. Both acetate and butyrate, have known cardiometabolic functions and neuroprotective effects respectively (Park and Sohrabji, 2016; Liu, 2021; Liu, 2020).

Plasma levels of acetate, which is the most abundant SCFA, were low at the acute phase (Fig. 12Ci) and increased by 10 %-20 % at 30d (Fig. 12Cii) (main effect of time, $F_{(1,37)}$: 55.1, p < 0.0001). At 2d post stroke, acetate levels were decreased by MCAo + vehicle compared to sham (p = 0.0002), and MCAo + IP-IGF1 (p = 0.0132). During the chronic phase, IP IGF1 treatment resulted in higher levels of this SCFA as compared to sham (p = 0.0017) and a trending increase compared to vehicle-treated MCAo animals (p = 0.0579).

In the case of butyrate, there was also an increase in this SCFA at the chronic phase (30d post stroke; Fig. 12Dii) as compared to the acute phase (2d post stroke; Fig. 12Di) in the IP study (main effect of time $F_{(1,34)}$: 32.28, p < 0.0001). At the acute time point, IP-IGF treated MCAo animals had higher levels of butyrate compared to the vehicle (p = 0.045). In the chronic phase there was no treatment or stroke effect. Taken together, these data indicate that IP-IGF1 treatment regulates acetate levels and increases butyrate levels during the acute phase.

SCFAs were also measured in stool samples collected 30d after stroke from the IP and ICV studies. There was no effect of either MCAo or IGF1 treatment observed in fecal SCFAs (Supplementary Fig 4).

7.15. Predictive modeling

In view of the cognitive impairment seem after stroke and its improvement by IP-IGF,

predictive modeling was used to determine whether gut microbes or metabolites.

could serve as indicators of stroke outcomes. Output measures included two features of the Barnes maze, time spent in the escape quadrant (probe trial) which is an estimate of recall, and latency to find the escape box, which is an estimate of learning.

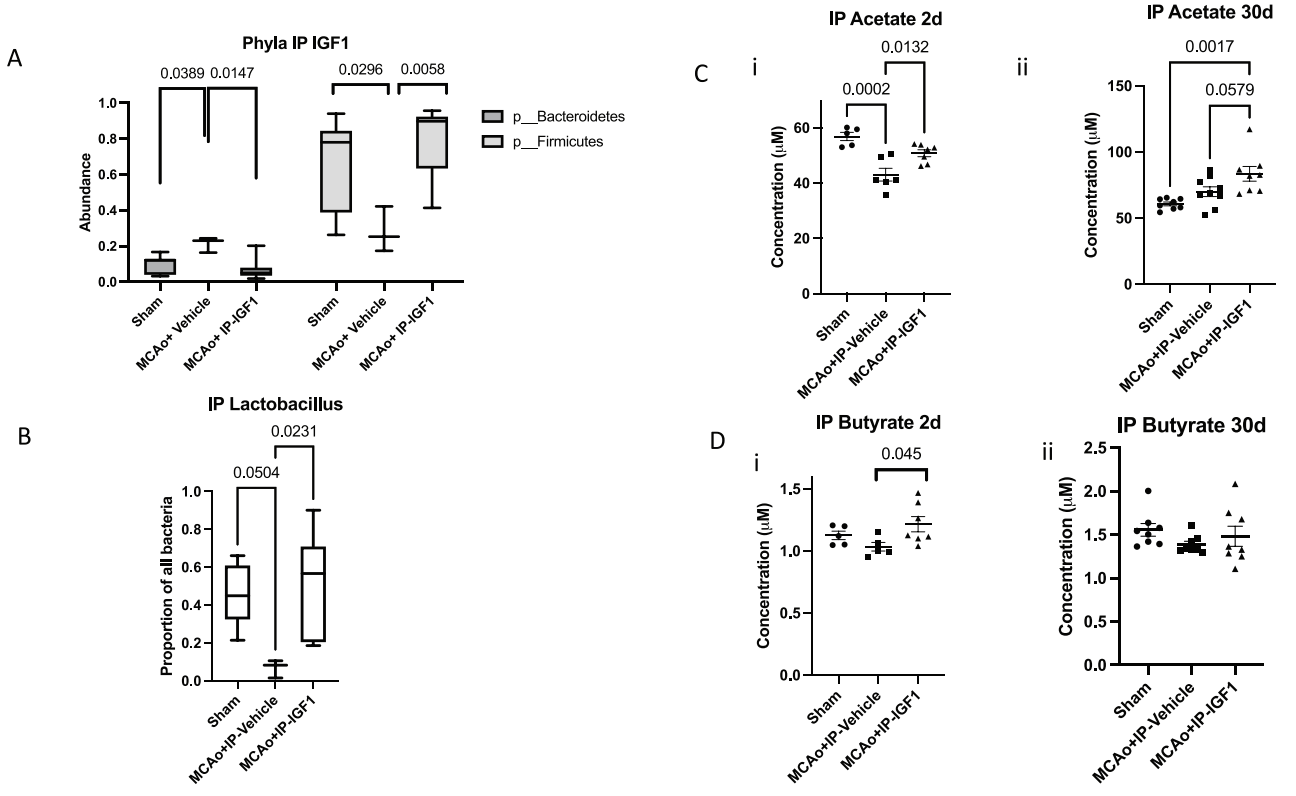

Fig. 12. *Assessment of gut dysbiosis and peripheral levels of SCFAs in the IP study*. A) Abundance of two major bacterial phyla (Firmicutes, Bacteroidetes) in fecal samples obtained 30d after MCAo. B) Relative abundance of selected species of the lactobacillus genus in the IP study. C) Plasma levels of acetate in the acute (2d) and chronic (30d) phase of the IP study. D) Plasma levels of butyrate in the acute (2d) and chronic (30d) phase of the IP study. All data analyzed by one way ANOVA with planned comparisons. n = 4–8/group. Exact p values for planned comparison as indicated in graphs.

7.15.1. Barnes probe trial as a response variable

Model estimates, 95 % confidence intervals, and *p* values for the logistic regression models for time spent in target quadrant response are shown in Table 1. LPS was significantly associated with Barnes probe trial (p = 0.0216), with an estimated coefficient that indicates a positive relationship between LPS and Probe trial. Additionally, the abundance of lactobacillus showed a strong trend towards a positive relationship with probe trial performance (p = 0.0567).

7.15.2. Barnes latency as a response variable

Model estimates, 95 % confidence intervals, and *p* values for the logistic regression models for time spent in target quadrant response are shown in Table 2. Among the gut phyla, Bacteroidetes was significantly associated with longer probe trial times (p = 0.0389). Here also Lactobacillus showed a trend towards statistical significance (p = 0.0533), with a positive relationship.

8. Discussion

The present study shows that the route of drug administration after MCAo can profoundly influence stroke outcomes. Central (ICV) delivery of IGF1 resulted in robust neuroprotection by reducing infarct volume and improving sensory motor performance in the acute phase but failed to attenuate stroke-induced cognitive impairment in the chronic phase. In contrast, systemic (IP) delivery of IGF1 showed a diametrically opposite effect; with no improvement of acute outcomes but robust amelioration of stroke-induced cognitive impairment in the chronic phase. The long-term stroke recovery seen in the IP-IGF1 study raises the possibility that the peptide may cross the stroke-damaged blood brain barrier and enter the brain. However, IP-delivered IGF-1 was not detected in the brain, and suggests instead that the peptide acts peripherally, on immune organs or their secretions, to prevent secondary neurodegeneration. This latter hypothesis is supported by studies showing that stroke promotes the trafficking of gut immune cells to the central nervous system (Brea, 2021), although it remains to be studied if IP-IGF1 abrogates this transfer of cells.

While ICV IGF1 treatment resulted was very neuroprotective in the acute phase, this did not have lasting effects. In preclinical studies, exogenous IGF-1 delivered intravenously (Rizk et al., 2007), intracerebroventricularly (icv), intranasally and via adeno-assisted virus delivery (Lin et al., 2009), reduces ischemic injury in many species (Gluckman, 1992; Guan et al., 2001; Johnston et al., 1996; Yan et al., 2006), stimulate stroke-induced neurogenesis (Yan et al., 2006), angiogenesis, myelination and neuronal survival (Smith, 2005; Wang, 2000). Our previous studies have shown that in addition to reduced infarction, icv-IGF-1 reduces permeability of the blood brain barrier (BBB) and neuroinflammation (Bake et al., 2014; Bake et al., 2019; Okoreeh et al., 2017) in middle-aged female rats. However, this advantage does not persist in the chronic phase, where volumetric analysis shows reduced ischemic hemisphere volume and enlarged ventricular volume in both vehicle and ICV-IGF1 treated animals. One possible explanation for this transient, but not persistent, neuroprotective effect of ICV-IGF1 is that ICV-IGF1 fails to attenuate peripheral inflammatory mediators such as IL-6, IL-17A and TNF-α that are elevated by stroke in both vehicle and ICV-IGF-1 groups in the acute phase and a persistent elevation of LPS at 30d after stroke. This peripheral inflammatory environment may exacerbate ongoing secondary neurodegeneration and is consistent with the poor performance on cognitive tests. IL-17A, for example, activates microglia, the brain resident macrophage, causing this cell type to initiate phagocytic activity. While microglial activation serves a critical purpose, chronic activation of this cell type may itself lead to further neuronal damage and loss of myelinated pathways, through the release of proinflammatory cytokines, proteinases and complement proteins. It is worth noting that IP-IGF1 treatment abrogates stroke-induced elevation of these cytokines in the acute phase and LPS in the chronic phase, thus potentially reducing on-going loss of neurons and myelin. This hypothesis receives some support from analysis of callosal thickness in the IP study, which is reduced in the vehicle group as compared to both sham and IP-IGF1 treated animals.

Table 1
Estimates, confidence intervals, and p values for the linear regression models for Barnes probe trial.

Coefficient	Explanatory Variable	Estimate	95 % CI (asymptotic)	P value
β0	Intercept	−1.412	−44.35 to 41.53	0.9385
β1	Firmicutes	−25.24	−62.04 to 11.57	0.1444
β2	Bacteroidetes	52.48	−54.56 to 159.5	0.2755
β3	Lactobacillus	45.98	−1.796 to 93.75	**0.0567**
β4	LPS	3.612	1.383 to 5.840	**0.0074**
β5	Butyrate	−5.664	−30.62 to 19.29	0.5988
β6	Acetate	−0.2344	−0.6522 to 0.1835	0.2190

Table 2
Estimates, confidence intervals, and p values for the linear regression models for Barnes latency.

Coefficient	Explanatory Variable	Estimate	95 % CI (asymptotic)	P value
β0	Intercept	−13.05	−92.54 to 66.45	0.7019
β1	Firmicutes	−4.677	−72.81 to 63.46	0.8721
β2	Bacteroidetes	213.3	15.15 to 411.4	**0.0389**
β3	Lactobacillus	86.75	−1.687 to 175.2	**0.0533**
β4	LPS	1.768	−2.357 to 5.893	0.3347
β5	Butyrate	−13.07	−59.27 to 33.13	0.5147
β6	Acetate	−0.1298	−0.9033 to 0.6437	0.6956

Stroke results in cognitive impairment in a significant subset of patients, however, most preclinical studies have focused on acute neuroprotection including measures such as mortality and loss of brain tissue (Bake et al., 2014; Bake et al., 2019; Selvamani and Sohrabji, 2017; Branyan, 2022), based on the premise that limiting neural damage in the acute phase would attenuate long term cognitive impairment. However, data from several studies show that infarct size is not linearly correlated with function in the acute or long-term phase (Lim et al., 2021; Turner, 2016; Ospel, 2021). Recent studies combining lesion mapping, functional imaging, and the human brain connectome, show that injuries in disparate areas of the brain can result in the same symptoms. Reciprocally, similar-sized lesions in the same location may also result in variable symptoms. At the cellular level, blood brain barrier disruption, which is not easily visible by imaging, and/or microstructural alterations in white matter are also suggested as explanations for variations in cognitive outcomes. Doyle and Buckwalter have proposed that in addition to lesion size and location, dementia after stroke is related to the extent of neural inflammation, as well as systemic immune responses that amplify brain immune responses (Doyle and Buckwalter, 2020). Elevated peripheral levels of inflammatory cytokines has been linked to depression (Chan et al., 2019) and post stroke cognitive impairment (PSCI) (Kulesh et al., 2018) as well as neurodegenerative diseases such as Alzheimer's Disease (Bermejo, 2008). For example, IL-6 is elevated in stroke patients as compared to controls and positively correlated with stroke volume and a less favorable 1 year prognosis (Waje-Andreassen, 2005). IL-17A has been implicated in multiple human and animal stroke studies where it has also been shown to be a mediator of tissue damage (Swardfager et al., 2013). Stroke induced elevations of inflammatory cytokines may contribute to ongoing BBB disruption and white matter lesions. In parallel studies in the lab, we report that neurocognitive changes due to MCAo is accompanied by a decrease in the volume of large myelin tracts such as the corpus callosum in middle-aged females (Panta, 2020), and decreased volume of the ischemic hemisphere normalized to the non-ischemic hemisphere in middle-aged males (Sampath, 2023).

The current study strongly implicates the gut as a direct or

intermediary target for long-term benefit for stroke outcomes. Clinically, stroke patients experience a variety of gastrointestinal (GI) related complications such as GI hemorrhage, dysphasia and reduced GI motility (Schaller et al., 2006). Experimentally, the gut shows an immediate and significant response to stroke in the form of gut dysmorphology and permeability (El-Hakim, 2021) with worse stroke outcomes being associated with a worse gut response (El-Hakim, 2021; Mani, 2023). Intestinal barriers, including the epithelial barrier, the mucosal layer and the endothelial barrier, ensure that gut contents are partitioned from general circulation (Groschwitz and Hogan, 2009; Natividad and Verdu, 2013; Vancamelbeke and Vermeire, 2017). Damage to these barriers can increase extravasation of inflammatory gut contents, including gut resident immune cells (Brea, 2021). and microbiota, into circulation, with the potential to impair the blood brain barrier by disrupting endothelial tight junctions of the BBB (Huber, 2002; Wolburg, 2003; Zhou, 2014), and thus harm overall brain health. A loss of intestinal barrier integrity is implicated in systemic immune inflammation, including in metabolic disease and chronic neurologic diseases (Camara-Lemarroy et al., 2018; Mulak and Bonaz, 2015; Jiang et al., 2017; Shen and Ji, 2019) as well as acute conditions such as stroke (Stanley, 2016) and traumatic brain injury (Pan, 2019). Thus, compounds that stabilize gut barriers may be the key to reducing peripheral inflammation. Several biochemical and histological analyses from this study show that stroke impacts gut barriers and that IP-IGF1 either attenuates this damage or accelerates its repair.

Disruption of the intestinal barriers also leads to detrimental changes in the composition of resident microbes, and consequently, synthesis of beneficial gut metabolites. Multiple preclinical and human studies have shown that there is a change in gut microbiome composition (gut dysbiosis) post stroke (Xu, 2021; Haak, 2021; Singh, 2016; Yamashiro, 2017) (also reviewed in (Honarpisheh et al., 2022), including an overgrowth in the Bacteroidetes phyla (Yamashiro, 2017), as seen in this study as well. More recently, stroke effects have also been reported for the ileal microbiome (Stanley et al., 2018; Ge et al., 2022) although much less is known about this biome in human stroke patients due to the challenge of collecting this microbiome. Baseline age-related changes in the microbiome, fecal microbiome transfer, depleting the microbiome through antibiotic administration (Benakis, 2016) all influence stroke outcome (Spychala, 2018), indicating the functional link between stroke and gut health. Reciprocally, stroke also influences the microbiome, resulting in alterations in specific microbial populations and not simply total bacterial abundance (Benakis, 2020) including a decrease in SCFA producing bacteria (Tan, 2021; Lee, 2020). Butyrate, a well-studied SCFA, is an energy source for epithelial cells, has anti-inflammatory properties, regulates proliferation and differentiation (reviewed in (Guilloteau, 2010) and promote gut blood barrier integrity (Geirnaert, 2017). While IP-IGF1′s effect on butyrate levels do not necessarily mean that this is the intermediary responsible for the beneficial outcomes of the peptide, previous work from our lab has shown that sodium butyrate treatment itself improves stroke outcomes in middle-aged acyclic female rats (Park and Sohrabji, 2016). A linear regression analysis shows that microbial composition, but not SCFA (butyrate, acetate), is associated with cognitive outcomes. However, a more granular assessment of bacterial families/species is needed for predictive purposes. Nonetheless, these data collectively suggest that timely gut repair may prevent pathogenic bacteria from colonizing the gut and reducing the proportion of beneficial bacteria.

The present study design does not exclude the possibility that IGF1 may act on the gut indirectly, although several studies show that this peptide has direct actions on intestinal tissue. Intestinal epithelial cells express the IGF1 receptor (Van Landeghem, 2015) as well as cells in the crypt proliferative compartment (Van Landeghem, 2015). IGF1 reduces gut barrier permeability (Huang et al., 1993) and improves intestinal/mucosal structure and reduce bacterial translocation to the mesenteric lymph node in a burn injury model (Huang et al., 1993), in a carbon tetrachloride-induced model of liver cirrhosis (Lorenzo-Zúñiga, 2006) and after small bowel transplantation (Zhang, 1995). IGF1 is known to enhance the expansion of intestinal stem cells and epithelial regeneration under normal and pathologic (radiation) conditions (Van Landeghem, 2015), and may well play a similar role under ischemic conditions. Thus, while IGF1 may likely act directly on the gut in stroke injury, future studies will be needed to confirm this with cell-specific knock-down of intestinal IGFR.

This study adds to the growing literature that recovery from acute neural injury is possible through improving gut health, and reciprocally, that gut health can impact neurological function. Several psychiatric comorbidities are seen in patients with Inflammatory Bowel Disease (IBS), including anxiety disorders and mood disorders (Fadgyas-Stanculete et al., 2014) as well major CNS disorders such as Multiple sclerosis (MS), AD, and Parkinson's disease (PD) (reviewed in (El-Hakim et al., 2022). Patients with IBS have a 6-fold greater risk for dementia (Zhang, 2021). In addition to the data from this project, our recent study using intestinal epithelial stem cell (IESC) transplants, which facilitated repair of the gut epithelium and improved long term behavioral recovery after stroke (Mani, 2023), also supports the idea of the gut as a therapeutic target. Moreover, the evidence that IP IGF-1, which does not improve acute stroke outcomes, is paradoxically beneficial for long term stroke induced cognitive outcomes has significant implications for stroke therapy. Research on stroke neuroprotectants has had numerous translational failures, and while many factors may be responsible for this, one possibility is that most studies have focused exclusively on acute phase effects. As our studies show, acute phase neuroprotection may not always result in improvement in chronic stroke outcomes, which crucially affect the patients' quality of life.

CRediT authorship contribution statement

Yumna El-Hakim: Writing – original draft, Methodology, Investigation, Formal analysis, Data curation. **Kathiresh Kumar Mani:** Writing – review & editing, Methodology, Investigation, Formal analysis. **Kaylin A. Pickle:** Writing – review & editing, Formal analysis, Data curation. **Zara Akbari:** Formal analysis. **Nadia Samiya:** Investigation, Data curation. **Chloe Pham:** Investigation. **Gianna Salas:** Methodology, Investigation. **Rachel Pilla:** Investigation, Formal analysis, Data curation. **Farida Sohrabji:** Writing – review & editing, Supervision, Funding acquisition, Formal analysis, Conceptualization.

Declaration of Competing Interest

The authors declare that they have no known competing financial interests or personal relationships that could have appeared to influence the work reported in this paper.

Data availability

Data will be made available on request.

Acknowledgements

This work was supported by the RF1NS119872 to Farida Sohrabji; Yumna El-Hakim is supported by a generous gift from the WoodNext Foundation; Kathiresh Kumar Mani supported by AHA postdoctoral fellowship (Award ID 831331). We thank Dr. Souza, Director of the Behavioral Core (Department of Neuroscience and Experimental Therapeutics), supported by the Janelle and Joe Marek '57 Alzheimers Disease Research Fund, for advice and training on the Barnes Maze studies.

Appendix A. Supplementary data

Supplementary data to this article can be found online at https://doi.org/10.1016/j.bbi.2024.08.008.

References

Bake, S., Selvamani, A., Cherry, J., Sohrabji, F., 2014. Blood brain barrier and neuroinflammation are critical targets of IGF-1-mediated neuroprotection in stroke for middle-aged female rats. PLoS One 9, e91427.

Bake, S., Gardner, R., Tingling, J.D., Miranda, R.C., Sohrabji, F., 2017. Fetal Alcohol Exposure Alters Blood Flow and Neurological Responses to Transient Cerebral Ischemia in Adult Mice. Alcohol. Clin. Exp. Res. 41, 117–127. https://doi.org/10.1111/acer.13277.

Bake, S., Okoreeh, A., Khosravian, H., Sohrabji, F., 2019. Insulin-like Growth Factor (IGF)-1 treatment stabilizes the microvascular cytoskeleton under ischemic conditions. Exp. Neurol. 311, 162–172. https://doi.org/10.1016/j.expneurol.2018.09.016.

Balden, R., Selvamani, A., Sohrabji, F., 2012. Vitamin D deficiency exacerbates experimental stroke injury and dysregulates ischemia-induced inflammation in adult rats. Endocrinology 153, 2420–2435. https://doi.org/10.1210/en.2011-1783.

Benakis, C., et al., 2016. Commensal microbiota affects ischemic stroke outcome by regulating intestinal γδ T cells. Nat. Med. 22, 516–523. https://doi.org/10.1038/nm.4068.

Benakis, C., et al., 2020. Distinct Commensal Bacterial Signature in the Gut Is Associated With Acute and Long-Term Protection From Ischemic Stroke. Stroke 51, 1844–1854. https://doi.org/10.1161/strokeaha.120.029262.

Bermejo, P., et al., 2008. Differences of peripheral inflammatory markers between mild cognitive impairment and Alzheimer's disease. Immunol. Lett. 117, 198–202. https://doi.org/10.1016/j.imlet.2008.02.002.

Bondanelli, M., et al., 2006. Predictive value of circulating insulin-like growth factor I levels in ischemic stroke outcome. J. Clin. Endocrinol. Metab. 91, 3928–3934. https://doi.org/10.1210/jc.2006-1040.

Branyan, T.E., et al., 2022. Functional Assessment of Stroke-Induced Regulation of miR-20a-3p and Its Role as a Neuroprotectant. Transl. Stroke Res. 13, 432–448. https://doi.org/10.1007/s12975-021-00945-x.

Brea, D., et al., 2021. Stroke affects intestinal immune cell trafficking to the central nervous system. Brain Behav. Immun. 96, 295–302. https://doi.org/10.1016/j.bbi.2021.05.008.

Bushnell, C.D., et al., 2014. Sex differences in quality of life after ischemic stroke. Neurology 82, 922–931. https://doi.org/10.1212/WNL.0000000000000208.

Bushnell, C., McCullough, L., 2014. Stroke prevention in women: synopsis of the 2014 American Heart Association/American Stroke Association guideline. Ann. Intern. Med. 160, 853–857. https://doi.org/10.7326/M14-0762.

Camara-Lemarroy, C. R., Metz, L., Meddings, J. B., Sharkey, K. A. & Wee Yong, V. The intestinal barrier in multiple sclerosis: implications for pathophysiology and therapeutics. *Brain : a journal of neurology* **141**, 1900-1916 (2018). https://doi.org/10.1093/brain/awy131.

Carrera, E., Tononi, G., 2014. Diaschisis: past, present, future. Brain J. Neurol. 137, 2408–2422. https://doi.org/10.1093/brain/awu101.

Challa, S.R., et al., 2024. The paradox of tPA in ischemic stroke: tPA knockdown following recanalization improves functional and histological outcomes. Exp. Neurol. 374, 114727 https://doi.org/10.1016/j.expneurol.2024.114727.

Chan, K.L., Cathomas, F., Russo, S.J., 2019. Central and Peripheral Inflammation Link Metabolic Syndrome and Major Depressive Disorder. Physiology (bethesda) 34, 123–133. https://doi.org/10.1152/physiol.00047.2018.

Corbett, D., Giles, T., Evans, S., McLean, J., Biernaskie, J., 2006. Dynamic changes in CA1 dendritic spines associated with ischemic tolerance. Exp. Neurol. 202, 133–138. https://doi.org/10.1016/j.expneurol.2006.05.020.

Donkor, E.S., 2018. Stroke in the 21(st) Century: A Snapshot of the Burden, Epidemiology, and Quality of Life. Stroke Res Treat 2018, 3238165. https://doi.org/10.1155/2018/3238165.

Doyle, K.P., Buckwalter, M.S., 2020. Immunological mechanisms in poststroke dementia. Curr. Opin. Neurol. 33, 30–36. https://doi.org/10.1097/wco.0000000000000783.

El-Hakim, Y., et al., 2021. Sex differences in stroke outcome correspond to rapid and severe changes in gut permeability in adult Sprague-Dawley rats. Biol. Sex Differ. 12, 14. https://doi.org/10.1186/s13293-020-00352-1.

El-Hakim, Y., Bake, S., Mani, K.K., Sohrabji, F., 2022. Impact of intestinal disorders on central and peripheral nervous system diseases. Neurobiol. Dis. 165, 105627 https://doi.org/10.1016/j.nbd.2022.105627.

Fadgyas-Stanculete, M., Buga, A.M., Popa-Wagner, A., Dumitrascu, D.L., 2014. The relationship between irritable bowel syndrome and psychiatric disorders: from molecular changes to clinical manifestations. J. Mol. Psychiatry 2, 4. https://doi.org/10.1186/2049-9256-2-4.

Gall, S.L., Tran, P.L., Martin, K., Blizzard, L., Srikanth, V., 2012. Sex differences in long-term outcomes after stroke: functional outcomes, handicap, and quality of life. Stroke 43, 1982–1987. https://doi.org/10.1161/STROKEAHA.111.632547.

Ge, Y., Zadeh, M., Yang, C., Candelario-Jalil, E., Mohamadzadeh, M., 2022. Ischemic Stroke Impacts the Gut Microbiome. Ileal Epithelial and Immune Homeostasis. *Iscience* 25, 105437. https://doi.org/10.1016/j.isci.2022.105437.

Geirnaert, A., et al., 2017. Butyrate-producing bacteria supplemented in vitro to Crohn's disease patient microbiota increased butyrate production and enhanced intestinal epithelial barrier integrity. Sci. Rep. 7, 11450. https://doi.org/10.1038/s41598-017-11734-8.

Gluckman, P., et al., 1992. A role for IGF-1 in the rescue of CNS neurons following hypoxic-ischemic injury. Biochem. Biophys. Res. Commun. 182, 593–599.

Groschwitz, K.R., Hogan, S.P., 2009. Intestinal barrier function: molecular regulation and disease pathogenesis. J. Allergy Clin. Immunol. 124, 3–22. https://doi.org/10.1016/j.jaci.2009.05.038.

Guan, J., Miller, O.T., Waugh, K.M., McCarthy, D.C., Gluckman, P.D., 2001. Insulin-like growth factor-1 improves somatosensory function and reduces the extent of cortical infarction and ongoing neuronal loss after hypoxia-ischemia in rats. Neuroscience 105, 299–306.

Guilloteau, P., et al., 2010. From the gut to the peripheral tissues: the multiple effects of butyrate. Nutr. Res. Rev. 23, 366–384. https://doi.org/10.1017/S0954422410000247.

Haak, B.W., et al., 2021. Disruptions of Anaerobic Gut Bacteria Are Associated with Stroke and Post-stroke Infection: a Prospective Case-Control Study. Transl. Stroke Res. 12, 581–592. https://doi.org/10.1007/s12975-020-00863-4.

Hackett, M.L., Pickles, K., 2014. Part I: frequency of depression after stroke: an updated systematic review and meta-analysis of observational studies. International Journal of Stroke : Official Journal of the International Stroke Society 9, 1017–1025. https://doi.org/10.1111/ijs.12357.

Honarpisheh, P., Bryan, R.M., McCullough, L.D., 2022. Aging Microbiota-Gut-Brain Axis in Stroke Risk and Outcome. Circ. Res. 130, 1112–1144. https://doi.org/10.1161/circresaha.122.319983.

Huang, K. F., Chung, D. H. & Herndon, D. N. Insulinlike growth factor 1 (IGF-1) reduces gut atrophy and bacterial translocation after severe burn injury. *Arch Surg* 128, 47-53; discussion 53-44 (1993). https://doi.org/10.1001/archsurg.1993.01420130051009.

Huber, J.D., et al., 2002. Blood-brain barrier tight junctions are altered during a 72-h exposure to lambda-carrageenan-induced inflammatory pain. Am. J. Phys. Heart Circ. Phys. 283, H1531–H1537. https://doi.org/10.1152/ajpheart.00027.2002.

Jacquin, A., et al., 2014. Post-stroke cognitive impairment: high prevalence and determining factors in a cohort of mild stroke. J. Alzheimers Dis. 40, 1029–1038. https://doi.org/10.3233/JAD-131580.

Jezierski, M.K., Sohrabji, F., 2001. Neurotrophin expression in the reproductively senescent forebrain is refractory to estrogen stimulation. Neurobiol. Aging 22, 309–319.

Jiang, C., Li, G., Huang, P., Liu, Z., Zhao, B., 2017. The Gut Microbiota and Alzheimer's Disease. Journal of Alzheimer's Disease : JAD 58, 1–15. https://doi.org/10.3233/jad-161141.

Johnsen, S.P., et al., 2005. Insulin-like growth factor (IGF) I, -II, and IGF binding protein-3 and risk of ischemic stroke. J. Clin. Endocrinol. Metab. 90, 5937–5941. https://doi.org/10.1210/jc.2004-2088.

Johnston, B.M., Mallard, E.C., Williams, C.E., Gluckman, P.D., 1996. Insulin-like growth factor-1 is a potent neuronal rescue agent after hypoxic-ischemic injury in fetal lambs. J. Clin. Invest. 97, 300–308. https://doi.org/10.1172/jci118416.

Kalaria, R.N., Akinyemi, R., Ihara, M., 2016. Stroke injury, cognitive impairment and vascular dementia. BBA 1862, 915–925. https://doi.org/10.1016/j.bbadis.2016.01.015.

Kulesh, A., Drobakha, V., Kuklina, E., Nekrasova, I., Shestakov, V., 2018. Cytokine Response, Tract-Specific Fractional Anisotropy, and Brain Morphometry in Post-Stroke Cognitive Impairment. J. Stroke Cerebrovasc. Dis. 27, 1752–1759. https://doi.org/10.1016/j.jstrokecerebrovasdis.2018.02.004.

Kumar, K.M., et al., 2017. Male reproductive toxicity of CrVI: In-utero exposure to CrVI at the critical window of testis differentiation represses the expression of Sertoli cell tight junction proteins and hormone receptors in adult F1 progeny rats. Reprod. Toxicol. 69, 84–98. https://doi.org/10.1016/j.reprotox.2017.02.007.

Lai, K.S.P., et al., 2017. Peripheral inflammatory markers in Alzheimer's disease: a systematic review and meta-analysis of 175 studies. J. Neurol. Neurosurg. Psychiatry 88, 876–882. https://doi.org/10.1136/jnnp-2017-316201.

Lee, J., et al., 2020. Gut Microbiota-Derived Short-Chain Fatty Acids Promote Poststroke Recovery in Aged Mice. Circ. Res. 127, 453–465. https://doi.org/10.1161/circresaha.119.316448.

Lim, J.S., Lee, J.J., Woo, C.W., 2021. Post-Stroke Cognitive Impairment: Pathophysiological Insights into Brain Disconnectome from Advanced Neuroimaging Analysis Techniques. J Stroke 23, 297–311. https://doi.org/10.5853/jos.2021.02376.

Lin, S., Fan, L.W., Rhodes, P.G., Cai, Z., 2009. Intranasal administration of IGF-1 attenuates hypoxic-ischemic brain injury in neonatal rats. Exp. Neurol. 217, 361–370. https://doi.org/10.1016/j.expneurol.2009.03.021.

Liu, J., et al., 2020. Anti-neuroinflammatory Effect of Short-Chain Fatty Acid Acetate against Alzheimer's Disease via Upregulating GPR41 and Inhibiting ERK/JNK/NF-kappaB. J. Agric. Food Chem. 68, 7152–7161. https://doi.org/10.1021/acs.jafc.0c02807.

Liu, J., et al., 2021. The Neuroprotective Effect of Short Chain Fatty Acids Against Sepsis-Associated Encephalopathy in Mice. Front. Immunol. 12, 626894 https://doi.org/10.3389/fimmu.2021.626894.

Liu, Z., Li, Y., Zhang, X., Savant-Bhonsale, S., Chopp, M., 2008. Contralesional axonal remodeling of the corticospinal system in adult rats after stroke and bone marrow stromal cell treatment. Stroke 39, 2571–2577. https://doi.org/10.1161/strokeaha.107.511659.

Lorenzo-Zúñiga, V., et al., 2006. Insulin-like growth factor I improves intestinal barrier function in cirrhotic rats. Gut 55, 1306–1312. https://doi.org/10.1136/gut.2005.079988.

Ma, Y., et al., 2019. Lactobacillus acidophilus Exerts Neuroprotective Effects in Mice with Traumatic Brain Injury. J. Nutr. 149, 1543–1552. https://doi.org/10.1093/jn/nxz105.

Mani, K.K., et al., 2023. Intestinal epithelial stem cell transplants as a novel therapy for cerebrovascular stroke. Brain Behav. Immun. 107, 345–360. https://doi.org/10.1016/j.bbi.2022.10.015.

Mellon, L., et al., 2015. Cognitive impairment six months after ischaemic stroke: a profile from the ASPIRE-S study. BMC Neurol. 15, 31. https://doi.org/10.1186/s12883-015-0288-2.

Mulak, A., Bonaz, B., 2015. Brain-gut-microbiota axis in Parkinson's disease. World J. Gastroenterol. 21, 10609–10620. https://doi.org/10.3748/wjg.v21.i37.10609.

Natividad, J.M.M., Verdu, E.F., 2013. Modulation of intestinal barrier by intestinal microbiota: Pathological and therapeutic implications. Pharmacol. Res. 69, 42–51. https://doi.org/10.1016/j.phrs.2012.10.007.
Okoreeh, A.K., Bake, S., Sohrabji, F., 2017. Astrocyte-specific insulin-like growth factor-1 gene transfer in aging female rats improves stroke outcomes. Glia 65, 1043–1058. https://doi.org/10.1002/glia.23142.
Ospel, J.M., et al., 2021. Strength of Association between Infarct Volume and Clinical Outcome Depends on the Magnitude of Infarct Size: Results from the ESCAPE-NA1 Trial. AJNR Am. J. Neuroradiol. 42, 1375–1379. https://doi.org/10.3174/ajnr.A7183.
Pan, P., et al., 2019. Intestinal barrier dysfunction following traumatic brain injury. Neurol. Sci. 40, 1105–1110. https://doi.org/10.1007/s10072-019-03739-0.
Panta, A., et al., 2020. Mir363-3p Treatment Attenuates Long-Term Cognitive Deficits Precipitated by an Ischemic Stroke in Middle-Aged Female Rats. Front. Aging Neurosci. 12, 586362 https://doi.org/10.3389/fnagi.2020.586362.
Panta, A., Pandey, S., Duncan, I.N., Duhamel, S., Sohrabji, F., 2019. Mir363-3p attenuates post-stroke depressive-like behaviors in middle-aged female rats. Brain Behav. Immun. 78, 31–40. https://doi.org/10.1016/j.bbi.2019.01.003.
Park, M.J., Sohrabji, F., 2016. The histone deacetylase inhibitor, sodium butyrate, exhibits neuroprotective effects for ischemic stroke in middle-aged female rats. J. Neuroinflammation 13, 300. https://doi.org/10.1186/s12974-016-0765-6.
Pendlebury, S.T., Rothwell, P.M., 2009. Prevalence, incidence, and factors associated with pre-stroke and post-stroke dementia: a systematic review and meta-analysis. The Lancet. Neurology 8, 1006–1018. https://doi.org/10.1016/s1474-4422(09)70236-4.
Poynter, B., et al., 2009. Sex differences in the prevalence of post-stroke depression: a systematic review. Psychosomatics 50, 563–569. https://doi.org/10.1176/appi.psy.50.6.563.
Rizk, N.N., Myatt-Jones, J., Rafols, J., Dunbar, J.C., 2007. Insulin like growth factor-1 (IGF-1) decreases ischemia-reperfusion induced apoptosis and necrosis in diabetic rats. Endocrine 31, 66–71.
Rosenfeld, C.S., Ferguson, S.A., 2014. Barnes maze testing strategies with small and large rodent models. J. vis. Exp. e51194 https://doi.org/10.3791/51194.
Sampath, D., et al., 2023. Sex differences in cognitive impairment after focal ischemia in middle-aged rats and the effect of iv miR-20a-3p treatment. Neurobiol. Aging 129, 168–177. https://doi.org/10.1016/j.neurobiolaging.2023.05.001.
Saver, J.L., et al., 2009. Stroke Therapy Academic Industry Roundtable (STAIR) recommendations for extended window acute stroke therapy trials. Stroke 40, 2594–2600. https://doi.org/10.1161/STROKEAHA.109.552554.
Schaller, B.J., Graf, R., Jacobs, A.H., 2006. Pathophysiological changes of the gastrointestinal tract in ischemic stroke. Am. J. Gastroenterol. 101, 1655–1665. https://doi.org/10.1111/j.1572-0241.2006.00540.x.
Selvamani, A., Williams, M. H., Miranda, R. C. & Sohrabji, F. Circulating miRNA profiles provide a biomarker for severity of stroke outcomes associated with age and sex in a rat model. *Clinical science (London, England : 1979)* **127**, 77-89 (2014). https://doi.org/10.1042/cs20130565.
Selvamani, A., Sohrabji, F., 2010. Reproductive age modulates the impact of focal ischemia on the forebrain as well as the effects of estrogen treatment in female rats. Neurobiol. Aging 31, 1618–1628. https://doi.org/10.1016/j.neurobiolaging.2008.08.014.
Selvamani, A., Sohrabji, F., 2017. Mir363-3p improves ischemic stroke outcomes in female but not male rats. Neurochem. Int. 107, 168–181. https://doi.org/10.1016/j.neuint.2016.10.008.
Shen, L., Ji, H.F., 2019. Associations Between Gut Microbiota and Alzheimer's Disease: Current Evidences and Future Therapeutic and Diagnostic Perspectives. Journal of Alzheimer's Disease : JAD 68, 25–31. https://doi.org/10.3233/jad-181143.
Singh, V., et al., 2016. Microbiota Dysbiosis Controls the Neuroinflammatory Response after Stroke. J. Neurosci. 36, 7428–7440. https://doi.org/10.1523/jneurosci.1114-16.2016.
Smith, L.E., 2005. IGF-1 and retinopathy of prematurity in the preterm infant. Biol. Neonate 88, 237–244. https://doi.org/10.1159/000087587.
Song, X., et al., 2022. Lactobacillus plantarum DP189 prevents cognitive dysfunction in D-galactose/AlCl(3) induced mouse model of Alzheimer's disease via modulating gut microbiota and PI3K/Akt/GSK-3beta signaling pathway. Nutr. Neurosci. 25, 2588–2600. https://doi.org/10.1080/1028415X.2021.1991556.
Spychala, M.S., et al., 2018. Age-related changes in the gut microbiota influence systemic inflammation and stroke outcome. Ann. Neurol. 84, 23–36. https://doi.org/10.1002/ana.25250.
Stanley, D., et al., 2016. Translocation and dissemination of commensal bacteria in post-stroke infection. Nat. Med. 22, 1277–1284. https://doi.org/10.1038/nm.4194.
Stanley, D., Moore, R.J., Wong, C.H.Y., 2018. An insight into intestinal mucosal microbiota disruption after stroke. Sci. Rep. 8, 568. https://doi.org/10.1038/s41598-017-18904-8.
Swardfager, W., et al., 2010. A meta-analysis of cytokines in Alzheimer's disease. Biol. Psychiatry 68, 930–941. https://doi.org/10.1016/j.biopsych.2010.06.012.
Swardfager, W., Winer, D.A., Herrmann, N., Winer, S., Lanctot, K.L., 2013. Interleukin-17 in post-stroke neurodegeneration. Neurosci. Biobehav. Rev. 37, 436–447. https://doi.org/10.1016/j.neubiorev.2013.01.021.
Tan, C., et al., 2021. Dysbiosis of Gut Microbiota and Short-Chain Fatty Acids in Acute Ischemic Stroke and the Subsequent Risk for Poor Functional Outcomes. JPEN J. Parenter. Enteral Nutr. 45, 518–529. https://doi.org/10.1002/jpen.1861.
Turner, R.C., et al., 2016. The role for infarct volume as a surrogate measure of functional outcome following ischemic stroke. J Syst Integr Neurosci 2. https://doi.org/10.15761/JSIN.1000136.
Van Landeghem, L., et al., 2015. IGF1 stimulates crypt expansion via differential activation of 2 intestinal stem cell populations. FASEB J. 29, 2828–2842. https://doi.org/10.1096/fj.14-264010.
Van Landeghem, L., et al., 2015. IGF1 stimulates crypt expansion via differential activation of 2 intestinal stem cell populations. FASEB J. 29, 2828–2842. https://doi.org/10.1096/fj.14-264010.
Vancamelbeke, M., Vermeire, S., 2017. The intestinal barrier: a fundamental role in health and disease. Expert Rev. Gastroenterol. Hepatol. 11, 821–834. https://doi.org/10.1080/17474124.2017.1343143.
Waje-Andreassen, U., et al., 2005. IL-6: an early marker for outcome in acute ischemic stroke. Acta Neurol. Scand. 111, 360–365. https://doi.org/10.1111/j.1600-0404.2005.00416.x.
Wang, J.M., et al., 2000. Reduction of ischemic brain injury by topical application of insulin-like growth factor-I after transient middle cerebral artery occlusion in rats. Brain Res. 859, 381–385.
Waters, D.L., Yau, C.L., Montoya, G.D., Baumgartner, R.N., 2003. Serum Sex Hormones, IGF-1, and IGFBP3 Exert a Sexually Dimorphic Effect on Lean Body Mass in Aging. J. Gerontol. A Biol. Sci. Med. Sci. 58, 648–652.
Wolburg, H., et al., 2003. Localization of claudin-3 in tight junctions of the blood-brain barrier is selectively lost during experimental autoimmune encephalomyelitis and human glioblastoma multiforme. Acta Neuropathol. 105, 586–592. https://doi.org/10.1007/s00401-003-0688-z.
Xu, K., et al., 2021. Rapid gut dysbiosis induced by stroke exacerbates brain infarction in turn. Gut. https://doi.org/10.1136/gutjnl-2020-323263.
Yamashiro, K., et al., 2017. Gut dysbiosis is associated with metabolism and systemic inflammation in patients with ischemic stroke. PLoS One 12, e0171521.
Yan, Y.P., Sailor, K.A., Vemuganti, R., Dempsey, R.J., 2006. Insulin-like growth factor-1 is an endogenous mediator of focal ischemia-induced neural progenitor proliferation. Eur. J. Neurosci. 24, 45–54. https://doi.org/10.1111/j.1460-9568.2006.04872.x.
Zhang, W., et al., 1995. Insulin-like growth factor-I improves mucosal structure and function in transplanted rat small intestine. Transplantation 59, 755–761. https://doi.org/10.1097/00007890-199503150-00020.
Zhang, B., et al., 2021. Inflammatory bowel disease is associated with higher dementia risk: a nationwide longitudinal study. Gut 70, 85–91. https://doi.org/10.1136/gutjnl-2020-320789.
Zhou, T., et al., 2014. Phospholipid transfer protein (PLTP) deficiency impaired blood-brain barrier integrity by increasing cerebrovascular oxidative stress. Biochem. Biophys. Res. Commun. 445, 352–356. https://doi.org/10.1016/j.bbrc.2014.01.194.